Available online at www.sciencedirect.com
SCIENCE DIRECT®
Journal of Organometallic Chemistry 690 (2005) 4285–4301
Journal of Organometallic Chemistry
www.elsevier.com/locate/jorganchem

Synthesis and structural characterization of *rac*-2-[(diphenylphosphino)methyl]ferrocenecarboxylic acid, its selected derivatives and some rhodium complexes

Martin Lamač, Ivana Císařová, Petr Štěpnička *

Department of Inorganic Chemistry, Faculty of Science, Charles University, Hlavova 2030, 128 40 Prague, Czech Republic

Received 4 January 2005; received in revised form 2 June 2005; accepted 2 June 2005
Available online 11 August 2005

Abstract

rac-2-[(Diphenylphosphino)methyl]ferrocenecarboxylic acid (**1**) was prepared in a good yield from *rac*-2-(*N*,*N*-dimethylaminomethyl)bromoferrocene (**2**) via *rac*-2-(hydroxymethyl)bromoferrocene (**4**) and *rac*-2-[(diphenylphosphino)methyl]bromoferrocene (**5**), and further converted to the respective phosphine oxide (**6**), phosphine sulfide (**7**) and methyl ester (**8**). The phosphines **1** and **8** were studied as ligands in rhodium complexes. The reaction of di-μ-chloro-bis[chloro-(η^5-pentamethylcyclopentadienyl)rhodium(III)] with the stoichiometric amounts of **1** and **8** yielded the corresponding mononuclear complexes with *P*-monodentate ligands: [$RhCl_2(\eta^5\text{-}C_5Me_5)$(L-κ*P*)], **9** and **10**, respectively. Attempted deprotonation of **9** with LiBu or KO*t*-Bu gave intractable mixtures, in which the parent complex **9** as the major component was accompanied by two new compounds, likely the diastereoizomeric phosphinocarboxylate complexes. A defined *O*,*P*-chelating phosphinocarboxylate complex, [*SP*-4-2]-carbonyl-[*rac*-2-{(diphenylphosphino)methyl}ferrocenecarboxylato-κ^2*O*,*P*]-tricyclohexylphosphinerhodium(I) (**12**), was obtained from the displacement of acetylacetonate(1−) (acac) ligand in [Rh(acac)(CO)(PCy_3)] (Cy = cyclohexyl) with acid **1**. The structures of **1**, **6** · $CHCl_3$, and **7** · 1/2CH_2Cl_2, **10**, and hydrated complexes **9** and **12** were determined by single-crystal X-ray diffraction.

Keywords: Hybrid ligands; Phosphines; Phosphinocarboxylic acids; Ferrocene; Rhodium; Crystal structure

1. Introduction

In spite of recent developments in the chemistry of phosphinoferrocene ligands [1], there is still only little known about ferrocene phosphines modified with polar functional groups [2]. In 1996, we reported the synthesis of 1′-(diphenylphosphino)ferrocenecarboxylic acid (Hdpf; see Chart 1) [3] – the first organometallic compound falling into the class of hybrid phosphinocarboxylic ligands [4]. Later studies revealed that whereas Hdpf coordinates usually as a simple phosphine [5], the respective carboxylate can bind transition metals as an *O*,*O*′-donor [6] or *O*,*P*-chelate [7]. Moreover, the acid and the respective methyl ester have been tested successfully as ligands in palladium-catalyzed Suzuki cross-coupling [8], and the acid was utilized as a modifier to MCM-41 with an aim of preparing supported catalysts [9].

More recently, we [10] and others [11] prepared the planarly chiral isomer of Hdpf, (S_p)-2-(diphenylphosphino)ferrocenecarboxylic acid (**A** in Chart 1), and used this chiral carboxyphosphine as a ligand in coordination compounds [10] and as a precursor for the synthesis of chiral ligands to be used in enantioselective catalysis [11a,11b,12]. As a continuation of our work on ferrocene carboxyphosphines, we turned to a formal homologue of

* Corresponding author. Fax: +420 221 951 253.
E-mail address: stepnic@natur.cuni.cz (P. Štěpnička).

0022-328X/$ - see front matter © 2005 Elsevier B.V. All rights reserved.
doi:10.1016/j.jorganchem.2005.06.035

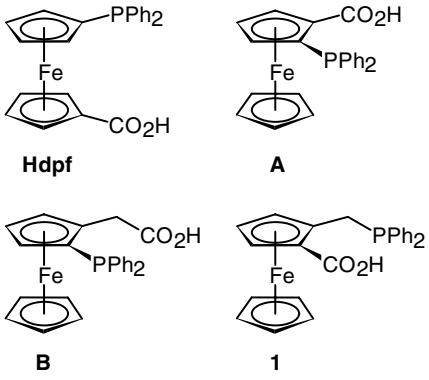

Chart 1.

the latter compound, *rac*-[2-(diphenylphosphino)ferrocenyl]acetic acid (**B**) [13]. A rather unique donor flexibility of ligand **B** and the corresponding methyl ester was demonstrated in a series of palladium(II) complexes, where the compounds behaved as *P*-monodentate phosphines, *O*,*P*-chelating ligands (**B** in the form of carboxylate) [13,14] and, after deprotonation of the ester at the activated methylene group, also as a *C*,*P*-chelating donor [15].

Considering the promising results obtained with compound **B**, we decided to prepare and study its isomer, *rac*-2-[(diphenylphosphino)methyl]ferrocenecarboxylic acid (**1**). In this contribution, we report on the synthesis and structural characterization of this ferrocene phosphinocarboxylic acid, its selected derivatives, and their rhodium complexes.

2. Results and discussion

2.1. Preparation and characterization of rac-[2-(diphenylphosphino)methyl]ferrocenecarboxylic acid and the derivatives

The preparation of the target ligand, *rac*-2-[(diphenylphosphino)methyl]ferrocenecarboxylic acid (**1**), is outlined in Scheme 1. The synthesis started from *rac*-2-(*N*,*N*-dimethylaminomethyl)bromoferrocene (**2**), which is accessible in a good yield from (*N*,*N*-dimethylaminomethyl)ferrocene by *ortho*-metallation and bromination with 1,2-dibromo-tetrafluoroethane as reported in the literature [16]. Bromoamine **2** was then converted by heating in acetic anhydride to acetate **3** and the acetate hydrolyzed to alcohol **4**. The alcohol was obtained also directly by alkaline hydrolysis of the reaction mixture resulting from the acetylation reaction. This one-pot procedure proved more practical and better yielding (85% vs. 75% for the two-step procedure). Compounds **3** [17] and **4** [18,17] have been already reported in the literature, but were synthesized by different methods. The solid-state structure of alcohol **4** is presented below.

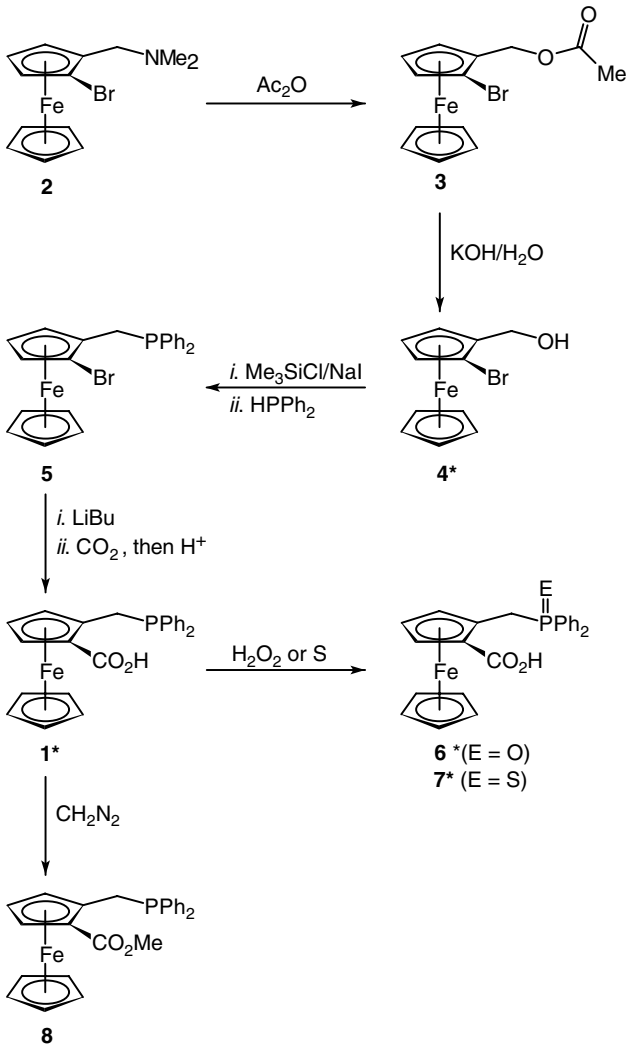

Scheme 1. Synthesis of carboxyphosphine **1** and the derivatives (the asterisk indicates that the solid state structure has been determined).

The subsequent preparation of phosphine bromide **5** proved rather difficult since neither bromoamine **2** nor the oxygen derivatives **3** and **4** reacted with diphenylphosphine to give the respective phosphinylated compound **5** under the reaction conditions described for the related 1-ferrocenylethyl derivatives [19]. It should be noted that in an early attempt at the preparation of **1**, we tried to replace similarly dimethylamino group in *rac*-2-[(dimethylamino)methyl]ferrocenecarboxylic acid with diphenylphosphine. However, the aminoacid, which itself was difficult to synthesize and purify due to its amphoteric nature (30% yield was obtained by using the procedure described for the synthesis of *rac*-2-[1-(dimethylamino)ethyl]ferrocenecarboxylic acid [20]), did not react with the phosphine either – even upon heating to 100 °C in glacial acetic acid.

Finally, the key intermediate **5** was obtained in an excellent yield directly from **4** by reacting the alcohol in acetonitrile with chlorotrimethylsilane/sodium iodide

and then with an excess of diphenylphosphine as it was recently described for related compounds by Šebesta [21]. As the last step, bromide **5** was lithiated with butyl lithium and the lithio intermediate carboxylated with carbon dioxide. A subsequent acidification gave the desired phosphinocarboxylic acid **1** in 73% yield after purification by column chromatography.

Furthermore, acid **1** was converted by the standard procedures to the corresponding phosphine oxide (**6**), phosphine sulfide (**7**) and methyl ester (**8**). All compounds were characterized by spectral methods, elemental analysis, and the structures of **1**, **6** · $CHCl_3$, and **7** · $1/2\,CH_2Cl_2$ have been determined by single-crystal X-ray diffraction (see below).

Compounds **1**–**8** are chiral, possessing an unsymmetrically 1,2-disubstituted ferrocene unit but were synthesized in the racemic form. Nevertheless, the chirality is reflected in the spectra. For instance, the presence of chirality plane makes the methylene protons diastereotopic and, hence, anisochronous. As a result, the methylene groups give rise to pairs of doublets in ^{1}H NMR spectra with the typical $^2J_{HH}$ coupling constants of ca. 12–15 Hz. For compounds **1** and **5**–**8**, these doublets are further split by an interaction with the directly bonded phosphorus groups. However, the extent of this interaction as reflected by the magnitude of the $^2J_{PH}$ coupling constants changes with the properties of phosphorus group and with the overall molecular geometry. For the mentioned series, the $^2J_{PH}$ values change from virtually no detected coupling in **5** and 1.3–1.5 Hz in the phosphines (**1** and **8**) to ca. 12–15 Hz for the compounds possessing pentavalent phosphorus groups (**6** and **7**).

The nature of the phosphorus group influences markedly also the ^{13}C NMR spectra. Apart from characteristic changes in the region of PPh_2 resonances (δ and J_{PC} values) [22], this concerns mainly the directly attached methylene group. Upon oxidation of carboxyphosphine **1** to the corresponding phosphine oxide or sulfide, the doublet due to the methylene group moves to lower field and the direct $^1J_{PC}$ constant increase from ca. 15 Hz (phosphines) to 67 Hz (**6**) and 49 Hz (**7**). ^{31}P NMR chemical shifts within the series **1** + **5**–**8** follow the expected trend [cf. −10.1 (**1** and **8**), 32.2 (**6**), 42.4 (**7**)]. However, the magnitude of the low field shift associated with oxidation of phosphines to P^V-compounds is significantly lower than in the homologous series derived from *rac*-2-[(diphenylphosphino)ferrocenyl]acetic acid (**B** in Chart 1). Besides, the ^{31} P NMR shift observed for **1** compares favourably with that of $FcCH_2PPh_2$ (−11.8, [23]).

IR spectra of the studied compounds are too complex for an unambiguous complete interpretation, an exception being the characteristic strong ν(C=O) bands in the spectra of the carboxylic derivatives **1** and **6**–**8**. The fact that the acids (**1**, **6**, **7**) show the ν(C=O) bands at relatively low frequencies can be ascribed to a synergism between conjugation of the carboxyl group with the ferrocene unit and hydrogen-bond formation in the solid state involving the carboxyl groups (see discussion of the crystal structures below). Accordingly, the frequency observed for **1** (1661 cm^{-1}) is very similar to Hdpf (1666 cm^{-1}, [3]), which has the carboxyl group attached directly to the ferrocene backbone and forms similar hydrogen bonded associates, and lower than for the isomeric acid **B** (1712 + 1695 sh cm^{-1} [13]), where the direct ferrocene-carboxyl conjugation is disrupted. The ν(C=O) band shifts to higher energies with increasing the electron withdrawing properties of the phosphorus substituent [ν(C=O): **1** < **7** < **6**]; esterification has a similar but more pronounced effect (**8**: 1704 cm^{-1}).

Electron-impact mass spectra of **1**–**8** show fragment ions typical for ferrocene compounds, e.g., those resulting from Fe–cyclopentadienyl bond cleavage such as $[C_5H_5Fe]^+$ and Fe^+ (for complete data, see Section 4). In addition, there are observed fragments specific for the individual compounds. Thus, acetate **3** fragments via a (formal) loss of C_6H_5Br, giving ions at *m*/*z* 180, which can be most likely formulated as $[C_5H_5FeOAc]^{+\cdot}$, and further by the loss of cyclopentadienyl radical (→ *m*/*z* 115). A similar transfer of an oxygen group to iron was observed also for the respective alcohol: the molecular ion $\mathbf{4}^{+\cdot}$ fragments by elimination of bromine atom yielding fragment species at *m*/*z* 215, which further eliminate phenyl radical to give ions $[C_5H_5FeOH]^{+\cdot}$ (*m*/*z* 138) and, subsequently, cyclopentadienyl to give $[FeOH]^+$ (*m*/*z* 73). The transfer of oxygen groups to iron atom during electron impact-induced fragmentation is not unprecedented in ferrocene chemistry. For instance, ferrocenecarboxylic acid and its methyl ester fragment to ions $[C_5H_5FeOR]^{+\cdot}$ (R = H or Me) [24] and 1′-(diphenylphosphinoyl)ferrocenecarboxylic acid (HdpfO) produces $[Ph_2PC_5H_5FeOH]^{+\cdot}$ [25].

Fragmentation of phosphine bromide **5** differs from the above compounds, the major fragmentation pathways for **5** being eliminations of PhBr (→ *m*/*z* 306) or PPh_2 fragment (→ *m*/*z* 277/279; this species is observed also in the spectrum of **3**). The presence of the diphenylphosphino group is reflected mainly by the characteristic peaks at *m*/*z* 183, attributable to 9-phosphofluorene cations (formally $[PPh_2 - 2\,H]^+$, [26]).

Likewise, the mass spectrum of acid **1** shows ions resulting from C–P bond breakage (*m*/*z* 243, $[M - PPh_2]^+$; base peak) as well as the 'complementary' ions at *m*/*z* 183, originating from PPh_2 (see above). Besides, ions $\mathbf{1}^{+\cdot}$ decompose by a simultaneous elimination of $CO_2 + C_6H_6$ (→ *m*/*z* 306). Decarboxylation of fragment ions at *m*/*z* 243 very likely gives rise to ferrocenylmethylium cation, $[FcCH_2]^+$ (or its isomeric form) at *m*/*z* 199.

The corresponding phosphine oxide ($\mathbf{6}^{+\cdot}$) fragments by a loss of cyclopentadienyl radical to give ions at *m*/*z*

379. In addition, the molecular ion and the ions at *m*/*z* 379 decarboxylate to give fragments at *m*/*z* 400 and 335, respectively. Analogous fragmentation pathways are the major fragmentation processes for phosphine sulfide **7**. In addition, the sulfide fragments by elimination of sulfur atom from the molecular ion, giving ions isobaric (and likely isostructural) with $\mathbf{1}^{+\cdot}$, which further decompose as described above for the acid.

Similarly to the parent acid, the spectra of ester **8** are dominated by ions at *m*/*z* 257, resulting from an elimination of the diphenylphosphino group, which in turn gives rise to fragments at *m*/*z* 183. The ions at *m*/*z* 257 are homologues to the ions at *m*/*z* 243 observed in the spectrum of the parent acid and apparently relate to the ions at *m*/*z* 227/229 observed in the spectrum of **3**.

2.2. The solid-state structures of *4*, *1*, *6* · $CHCl_3$, and *7* · *1/2*CH_2Cl_2

As mentioned above, the compounds studied are racemic and crystallize to form racemic crystals with the symmetry of centrosymmetric space groups. Among the structurally characterized compounds, alcohol **4** is an exception, crystallizing with two molecules in the asymmetric unit (*C*2/*c* space group; two molecules with (S_p) configuration were chosen arbitrarily for the refinement). Geometric parameters for the independent molecules (Fig. 1(a), Table 1) differ only very marginally, e.g., in tilt of the cyclopentadienyl (Cp) rings and in torsion angles at C(Cp)–C(OH) bond, the latter specifying the orientation of the flexible hydroxymethyl side arm towards its parent cyclopentadienyl ring. Besides, the molecules differ in conformation of the ferrocene unit: the cyclopentadienyl rings in molecules 1 and 2 are rotated by ca. 3° and 36°, which indicates a near-to-eclipsed and a perfectly staggered conformation, respectively. Considering such minimum differences between the molecules, the increase in the number of symmetrically independent molecules should be sought in intermolecular association. The molecules associate predominantly by means of O–H···O interactions so that each hydroxyl group acts as both the hydrogen bond donor and acceptor, forming infinite helical chains parallel to the crystallographic *b*-axis (Fig. 1(b), Table 2). The individual chains involve molecules with the same configuration [(R_p) or (S_p)] and, consequently, the unit cell accommodates two pairs of chains differing only by their polarity. The O···O separations of ca. 2.75 Å compare favourably with the values observed for *rac*-[2-(diphenylphosphino)ferrocenyl]methanol (2.751(3) Å, [27]) and are shorter than those in [1′-(diphenylphosphino)ferrocenyl]methanol (2.835(4)–2.866(4) Å, [28]).

The molecular structures of the acids differ only at the phosphorus substituent. Therefore, structural parameters for **1** and the solvates **6** · $CHCl_3$ and **7** · 1/2CH_2Cl_2 will be discussed jointly. Views of the molecular structures are shown in Figs. 2–4 and the relevant structural data are listed in Table 3. The arrangement of the ferrocene units in the acids is quite regular: the iron-ring centroid distances for both cyclopentadienyl ring differ by less than 0.5% and the ring tilts are lower than 5°. Notably, acid **1** exhibits a significant torsion at the C(1)–C(2) bond whereas its phosphinoyl and thiophosphoryl derivatives bearing bulkier phosphorus groups show only negligible such deformation. In all compounds, the rotation of the carboxyl group from the least-squares plane of the substituted cyclopentadienyl ring does not exceed 15° and the carboxyl group is oriented so that the C=O bond points to the methylene arm.

Steric demands of the phosphorus group increasing in the order **1** (lone pair) > **6** (O) > **7** (S) are reflected by an opening of the C(2)–C(12)–P angle. In the same order, the angle subtended by the P–C(12) bond and the Cp1

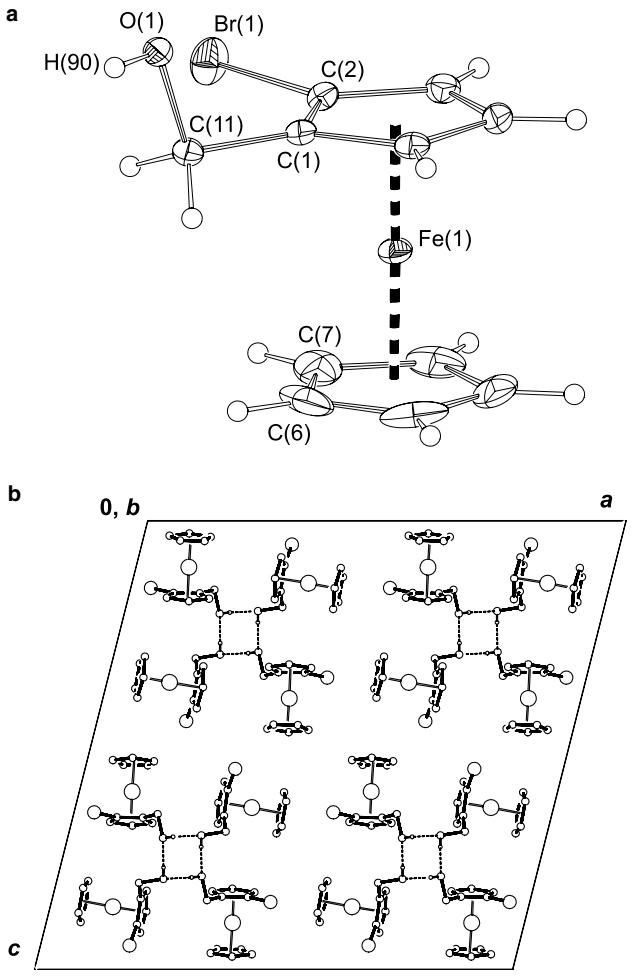

Fig. 1. (a) A view of the molecular structure of molecule 1 in the structure of alcohol **3**. Thermal motion ellipsoids enclose 30% probability. The respective atom labels for molecule 2 are obtained by adding 20 [except for Fe(2), Br(2), O(2) and H(92)]. (b) Crystal packing of **3** as viewed along the crystallographic *b*-axis showing the hydrogen bonds as dashed lines. Hydrogen atoms except those at OH groups are omitted for clarity.

Table 1
Selected distances and angles for **4** (in Å and °)[a]

Molecule 1		Molecule 2	
Fe–Cg1	1.636(1)	Fe–Cg3	1.639(1)
Fe–Cg2	1.652(2)	Fe–Cg4	1.651(2)
∠Cp1,Cp2	2.0(2)	∠Cp3,Cp4	0.9(2)
C(1)–C(11)	1.483(4)	C(21)–C(31)	1.489(4)
C(11)–O(1)	1.436(3)	C(31)–O(2)	1.439(3)
Br(1)–C(2)	1.889(3)	Br(2)–C(22)	1.888(3)
C(1)–C(11)–O(1)	108.8(2)	C(21)–C(31)–O(2)	108.1(2)
C(2)–C(1)–C(11)	127.6(2)	C(22)–C(21)–C(31)	127.8(2)
C(2)–C(1)–C(11)–O(1)	−98.2(3)	C(22)–C(21)–C(31)–O(2)	−94.7(3)
C(11)–C(1)–C(2)–Br(1)	1.6(4)	C(31)–C(21)–C(22)–Br(2)	0.4(4)

[a] Ring definition: Cp1 = C(1–5), Cp2 = C(6–10), Cp3 = C(21–25), Cp4 = C(26–30). Cg denotes the respective ring centroid.

Table 2
Hydrogen bond parameters for **4**, **1**, **6** · $CHCl_3$, **7** · 1/2CH_2Cl_2 (in Å and °)[a]

D–H···A	D–H···A	D–H	D–H···A
Compound **4**			
O(1)–H(91)···O(2^{i})	2.746(3)	0.75(3)	178(6)
O(2)–H(92) · · O(1)	2.751(3)	0.71(3)	176(3)
Compound **1**			
O(2)–H(90)···O(1^{ii})	2.629(3)	0.88(6)	171(5)
Compound **6** · $CHCl_3$			
O(2)–H(90)···O(1^{iii})	2.646(2)	0.69(3)	176(3)
C(25)–H(25)···O(3^{iv})	2.976(2)	0.98	173
Compound **7** · 1/2CH_2Cl_2			
O(2)–H(90)···O(1^{v})	2.663(2)	0.85(4)	179(6)

[a] Values involving hydrogen atoms in geometrically defined positions are given without esd's. Symmetry operations: (i) 1/2 − *x*, *y* − 1/2, 1/2 − *z*; (ii) 1 − *x*, 1 − *y*, 1 − *z*; (iii) 1 − *x*, −*y*, −*z*; (iv) 1 + *x*, *y*, *z*; (v) −*x*, −*y*, 1 − *z*.

plane becomes more acute [76.3(2)°, 70.6(1)°, 67.2(1)°; N.B. only the angle between 0° and 90° is considered], though with only a minor change of the conformation at the C(2)–C(12) bond (see the C(1)–C(2)–C(12)–P torsional angles in Table 3).

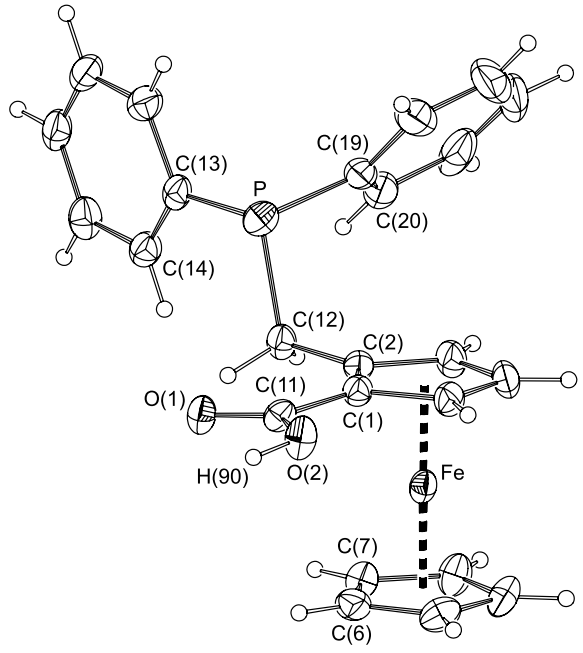

Fig. 2. A view of the molecular structure of acid **1**. Thermal motion ellipsoids are drawn at the 30% probability level.

In crystal, the acids associate into centrosymmetric hydrogen-bonded dimers connected by a pair of O–H···O=C hydrogen bonds (notation according to the graph set theory: $R_2^2(8)$ [29]). The O···O distances are virtually independent of the phosphorus group, differing relatively by only ca. 1% in the whole series (Table 2). Compounds **1**, **6**, and **7** thus parallel the behaviour of Hdpf (O···O ca. 2.65 Å for Hdpf [3] and complexes featuring *P*-coordinated Hdpf [5]) and **B** (O···O 2.646(2) Å [13]), which form similar supramolecular aggregates. The phosphinoyl oxygen atom in **6**, which is not involved in this interaction, forms additional hydrogen bonds to the solvating chloroform molecules: P=O···$HCCl_3$ (Fig. 5, Table 2), which fix the solvent molecules in the structure. On the other hand, the structure of solvate **7** · 1/2CH_2Cl_2 lacks similar interactions, very likely due to much worse hydrogen-bond acceptor properties of the sulfur atom. Consequently, the solvating dichloromethane is bonded only loosely in hydrophobic channels defined by the phenyl rings. The solid-state assemblies of the acids are further supported by graphitic π···π stacking of the phenyl rings and C–H···π interactions.

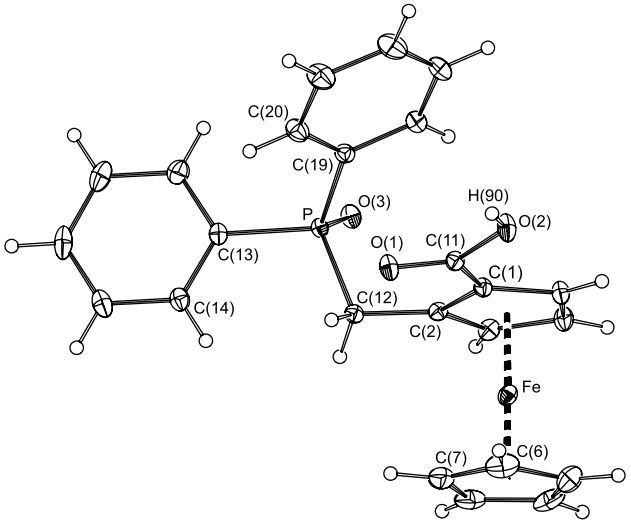

Fig. 3. The molecular structure of $\mathbf{6} \cdot CHCl_3$. For clarity, the solvate molecule is omitted. Thermal motion ellipsoids are drawn at the 30% probability level.

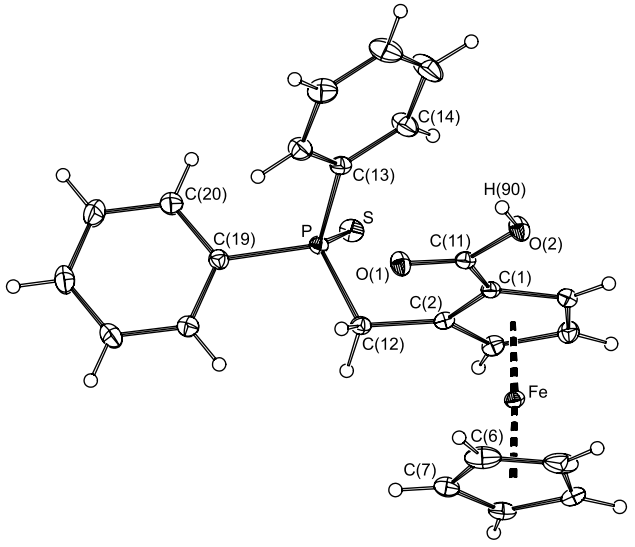

Fig. 4. A view of the molecular structure of $\mathbf{7} \cdot 1/2\,CH_2Cl_2$. Disordered solvate molecule are omitted. Thermal motion ellipsoids correspond to the 30% probability level.

2.3. Preparation and structures of (η^5-pentamethylcyclopentadienyl)rhodium(III) complexes

Cleavage of the chloro bridges in di-μ-chloro-bis-[chloro-(η^5-pentamethylcyclopentadienyl)rhodium(III)] with the stoichiometric amounts of acid **1** and methyl ester **8** gave the corresponding (η^5-cyclopentadienyl)rhodium(III) complexes [$RhCl_2(\eta^5$-$C_5Me_5)$(**1**-κ*P*)] (**9**) and [$RhCl_2(\eta^5$-$C_5Me_5)$(**8**-κ*P*)] (**10**), where the ferrocene ligands bind as monodentate phosphines (Scheme 2). The complexes were characterized by IR and NMR spectra and their structures corroborated by single-crystal X-ray diffraction. Exclusive *P*-coordination of the ligands is best reflected by ^{31}P NMR spectra, where the ligand signals are shifted to lower fields (coordination shifts: Δ_P 45.2 (**9**), 45.1 (**10**)) and show characteristic coupling with ^{103}Rh ($I = 1/2$, 100% abundance; $^1J_{RhP}$ ca. 140 Hz). On the other hand, ^{13}C NMR resonances

Table 3
Selected distances and angles for **1**, $\mathbf{6} \cdot CHCl_3$, and $\mathbf{7} \cdot 1/2\,CH_2Cl_2$ (in Å and °)[a]

Parameter	**1**	$\mathbf{6} \cdot CHCl_3$	$\mathbf{7} \cdot 1/2\,CH_2Cl_2$
E	Void	O(3)	S
Fe–Cg1	1.644(2)	1.6475(9)	1.644(1)
Fe–Cg2	1.651(2)	1.656(1)	1.649(1)
∠Cp1,Cp2	0.1(2)	4.4(1)	2.7(2)
C(1)–C(11)	1.462(4)	1.460(3)	1.459(3)
C(11)–O(1)	1.233(4)	1.232(2)	1.228(3)
C(11)–O(2)	1.313(4)	1.315(2)	1.322(3)
C(2)–C(12)	1.502(5)	1.498(3)	1.497(3)
P–C(12)	1.861(4)	1.817(2)	1.828(2)
P–C(13)	1.828(4)	1.807(2)	1.817(2)
P–C(19)	1.828(4)	1.801(2)	1.816(3)
P=E	–	1.493(1)	1.9588(9)
O(1)–C(11)–O(2)	123.1(3)	122.9(2)	122.7(2)
C(2)–C(12)–P	107.7(2)	110.6(1)	112.4(2)
C–P–C[b]	98.6(2)–105.0(2)	105.55(8)–107.05(9)	104.7(1)–106.0(1)
C–P–E[c]		112.16(8)–112.63(8)	112.49(8)–114.33(8)
C(1)–C(2)–C(12)–P	87.6(4)	93.6(2)	92.5(2)
C(11)–C(1)–C(2)–C(12)	12.9(6)	1.5(3)	3.8(4)
∠COO,Cp1[d]	5.4(4)	12.9(2)	9.3(3)

[a] Definitions of the ring planes: Cp1 = C(1–5), Cp2 = C(6–10), Cg1 and Cg2 are the respective ring centroids.
[b] The range of C(12)–P–C(13,19) and C(13)–P–C(19) angles.
[c] The range of C(12,13,19)–P–E angles.
[d] Dihedral angle of the Cp1 and carboxyl [C(11)O(1)O(2)] planes.

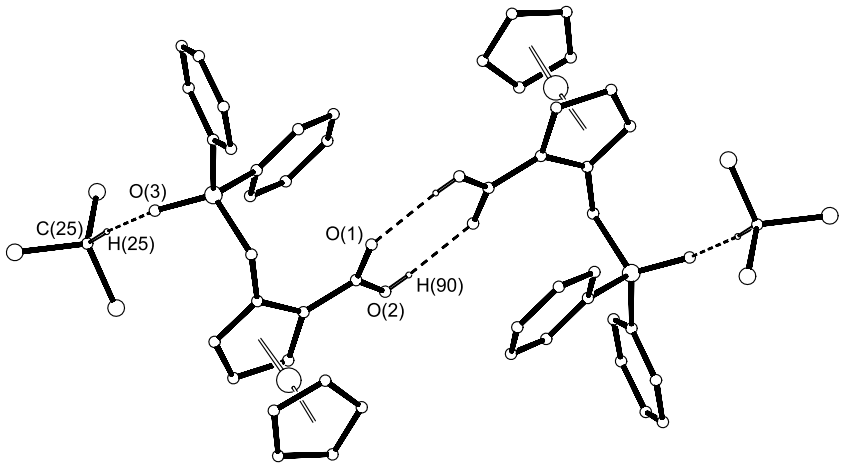

Fig. 5. A schematic drawing of the hydrogen bonded aggregates in the structure of $\mathbf{6} \cdot CHCl_3$.

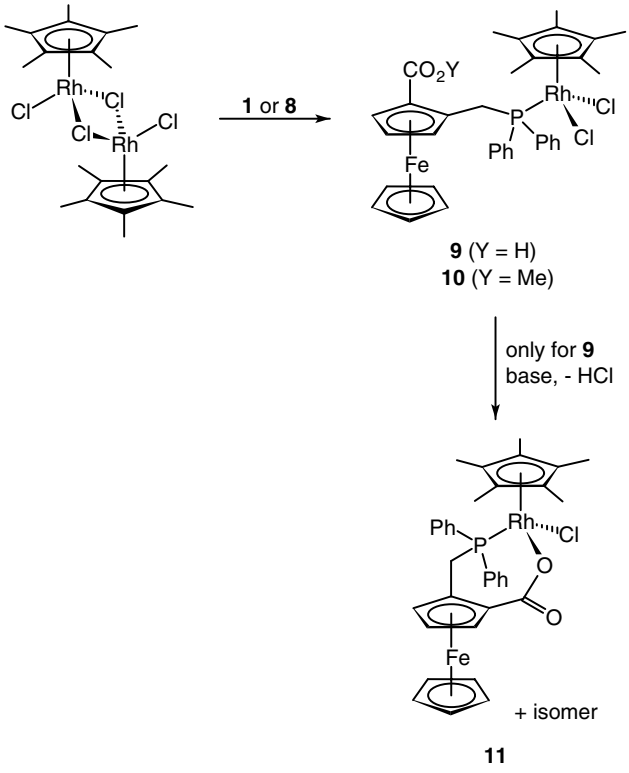

Scheme 2. Preparation of (η^5-cyclopentadienyl)rhodium(III) complexes.

of the carboxylic carbons as well as carbonyl stretching bands in IR spectra shift upon coordination only very slightly, thus excluding any significant involvement of the carboxyl moieties in coordination to the rhodium centres.

Attempts to synthesize a phosphinocarboxylate complex by deprotonation of **9** with bases such as KO*t*Bu or LiBu failed. According to NMR spectra (see Section 4), the reaction mixtures contained the parent complex **9** (major) and two new compounds, likely attributable to the diastereoisomers of the formed phosphinocarboxylate complex **11** (Scheme 2) [30]. Unfortunately, all attempts to purify the reaction mixtures by crystallization or chromatography were unsuccessful.

The molecular structures of **9** and **10** as determined by X-ray crystallography are shown in Figs. 6 and 7, respectively, while the pertinent geometric data are summarized in Table 4. Complex **9** crystallized from aqueous acetic acid as an ill-defined hydrate, having the solvating molecules located in a space close to the polar carboxyl groups (see Section 4).

The molecules of the complexes are very similar, adopting the expected three-legged piano stool geometry. In both cases, the phosphinocarboxylic ligand is coordinated only via the phosphino group and its phenyl rings are orientated towards the pentamethylcyclopentadienyl (Cp*) ring. The respective dihedral angles are: Ph vs. Cp3 29.5(2)° and 29.4(2)° for **9**, and 14.1(2)° and 39.1(2)° for **10** (see Table 4 for the definition of the ring planes). The ferrocene moieties are directed to the other side of the Cp*Rh unit and rotated with respect to the Cp* plane (cf. dihedral angle Cp1 vs. Cp3: 50.3(2)° for **9** and 42.6(3)° for **10**). The coordination spheres around the rhodium(III) atoms in both compounds show noticeable deformations: the Cg3–Rh–P angles are by ca. 10° less acute than the Cg3–Rh–Cl(1,2) angles. However, this deformation, which apparently results from the steric demands of the phosphine group, causes virtually no slanting to the [Cp*RhL_3] unit (cf. the dihedral angles subtended by the Cp3 and [PCl(1)Cl(2)] planes of 4.3(1)° and 3.8(1)°, respectively).

As far as the geometry of the phosphinocarboxylic ligand is concerned, the coordination influences the arrangement of the phosphine substituent only, leaving the rest of the ligand molecule nearly intact. The ligands are coordinated without any deformation to the ferrocene unit and torsion at the C(1)–C(2) bond (see data in Table 4). Coordination of the diphenylphosphino

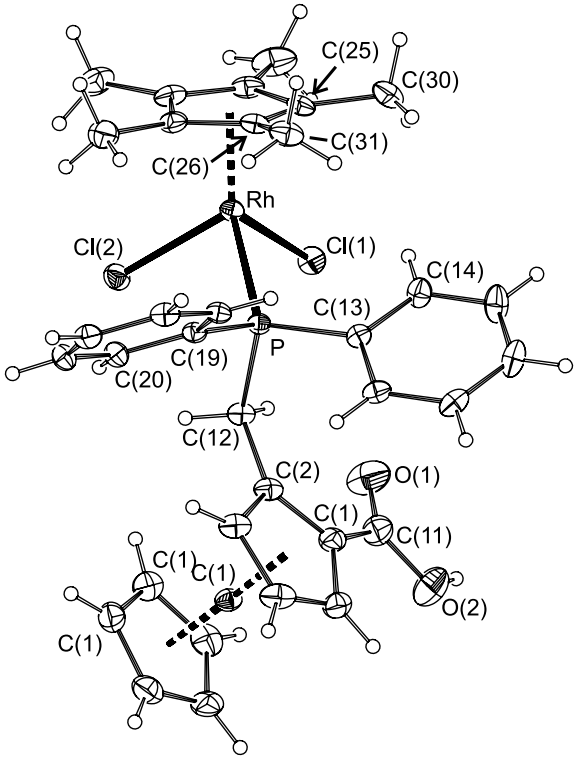

Fig. 6. The molecular structure of **9** (the solvate molecules are not shown). Thermal motion ellipsoids are drawn at the 30% probability level.

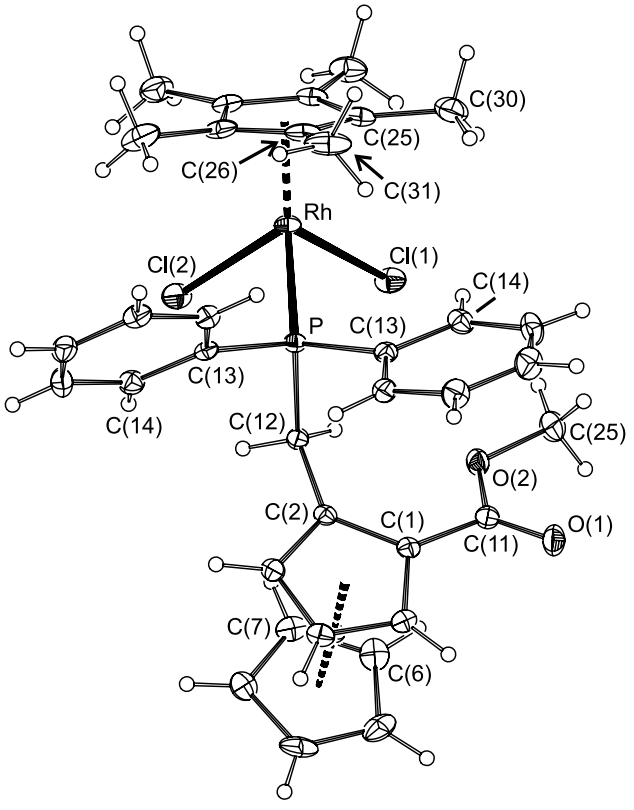

Fig. 7. A view of the molecular structure of **10**. Thermal motion ellipsoids are drawn at the 30% probability level.

Table 4
Selected distances and angles for **9** and **10** (in Å and °)[a]

Parameter	**9** (hydrate)	**10**
Rh–Cl(1)	2.4038(9)	2.4070(7)
Rh–Cl(2)	2.4125(9)	2.4060(8)
Rh–P	2.3326(8)	2.3159(7)
Rh–Cg3	1.814(2)	1.815(1)
Cg3–Rh–Cl(1)	122.51(5)	121.34(5)
Cg3–Rh–Cl(2)	121.34(5)	123.29(5)
Cg3–Rh–P	132.62(5)	132.22(4)
Cl(1)–Rh–Cl(2)	91.76(3)	92.69(3)
P–Rh–Cl(1)	89.44(3)	90.89(2)
P–Rh–Cl(2)	87.66(3)	84.96(3)
Fe–Cg1	1.640(2)	1.644(1)
Fe–Cg2	1.645(2)	1.650(2)
∠Cp1,Cp2	2.7(2)	1.6(2)
C(1)–C(11)	1.461(5)	1.466(4)
C(11)–O(1)	1.221(5)	1.210(3)
C(11)–O(2)	1.327(5)	1.338(4)
O(2)–C(35)		1.446(4)
C(2)–C(12)	1.498(5)	1.496(4)
P–C[b]	1.823(3)–1.849(3)	1.824(3)–1.853(2)
O(1)–C(11)O(2)	121.7(4)	123.9(3)
C(2)C(12)–P	115.8(2)	115.8(2)
C–P–C[c]	104.2(2)–105.6(1)	103.1(1)–107.4(1)
C(1)–C(2)–C(12)–P	111.4(3)	−90.6(3)
C(11)–C(1)–C(2)–C(12)	−6.9(5)	−1.3(4)
∠Cp1,COOH	6.7(5)	16.3(3)

[a] Definition of the ring planes: Cp1 = C(1–5), Cp2 = C(6–10), Cp3 = C(25–29). Cg(1–3) stand for the respective ring centroids. COOH is the carboxyl plane [C(11)O(1)O(2)]
[b] The range of P–C(12,13,19) distances.
[c] The range of C(12)–P–C(13,19) and C(13)–P–C(19) angles.

group results in tetrahedrally surrounded phosphorus atoms, which in turn causes an opening of the C–P–C angles, similarly to oxidation of **1**–**6** or **7** (compare data in Tables 3 and 4). Correspondingly, the C(1)–C(2)–P angles are more opened due to an increased bulk of the 'group' attached to the methylene spacer.

2.4. Preparation and structure of a rhodium(I) phosphinocarboxylate complex *12*

The reaction of carboxyphosphine **1** with the stoichiometric amount of rhodium(I)-acetylacetonato (acac) complex [Rh(acac)(PCy_3)(CO)] (Hacac = pentan-2,4-dione, Cy = cyclohexyl) proceeds with acid–base displacement of the acac ligand and formation of a chelating phosphinocarboxylate complex **12** (Scheme 3). Acid **1**

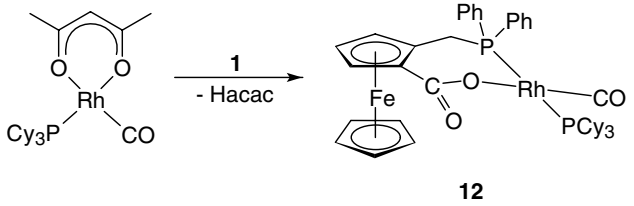

12

Scheme 3. Synthesis of the chelating phosphinocarboxylate complex **12**.

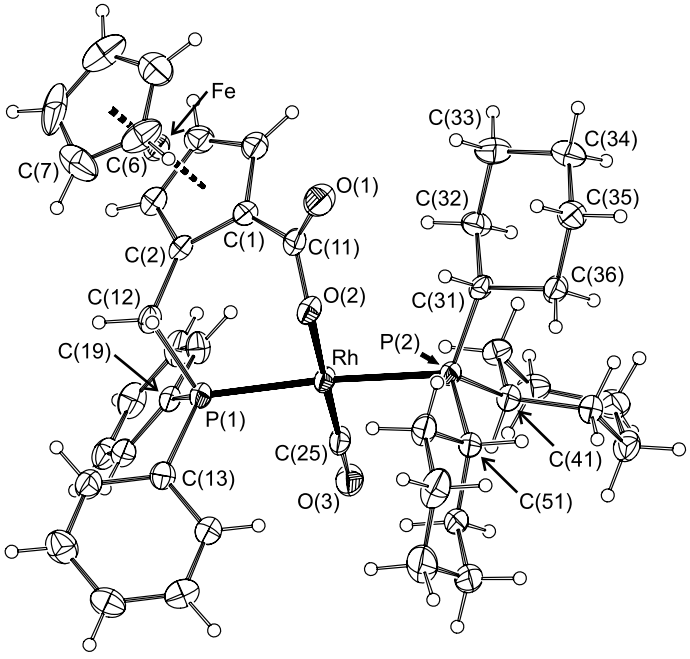

Fig. 8. The molecular structure of **12**. The solvate molecules are omitted for clarity. Thermal motion ellipsoids correspond to 30% probability level.

thus seemingly parallels the reactivity of (diphenylphosphino)acetic acid [31] and Hdpf [7]. The complex was characterized by standard spectral methods and elemental analysis. In ^{31}P NMR spectra, complex **12** exhibits a pair of double doublets at δ_P 32.8 (carboxylate) and 40.9 (PCy_3) with the characteristic $^1J_{RhP}$ (ca. 130 Hz) and $^2J_{PP}$ (322 Hz) coupling constants [32]. On the other hand, deprotonation and coordination of the carboxyl group is reflected by a low-shift of the ^{13}C NMR signal due the carboxyl group (δ_C 175.28) and, mainly, by a shift of the ν(C=O) band to lower energies (ca. 60 cm^{-1}).

Recrystallization of **12** from commercial methanol gives hydrates with varying water content. This corresponds with the solid-state structure of **12** · 0.7H_2O, which revealed that the water molecules are distributed rather freely in the crystal (though in hydrogen bond distances) in voids left between the bulky hydrophobic complex molecules, which itself are packed at the distances of the van der Walls contacts without further significant intermolecular contacts.

The molecular structure of **12** is shown in Fig. 8 and the pertinent geometric data are given in Table 5. Coordination sphere around rhodium is nearly perfectly planar, with the interligand angles deviating from 90° only very slightly. The individual Rh-donor distances are practically identical with the respective values in *trans*-[Rh(dpf-κ*O*,*P*)(PCy_3)(CO)] (Rh–P(dpf) 2.335(1), Rh–P(PCy_3) 2.342(1), Rh–O2.071(2), and Rh–CO 1.793(3) Å [7]) and *trans*-[Rh($Ph_2PCH_2CO_2$-κ*O*,*P*)($Ph_2PCH_2CO_2$-H-κ*P*)(CO)] (Rh–P(carboxylate) 2.302(2), Rh–P(acid) 2.346(2), Rh–O 2.064(6), and Rh–CO 1.77(1) Å [31a]). Likewise, the overall arrangements of the PCy_3 and carbonyl ligands are almost identical to those in the former reference compound.

Table 5
Selected distances and angles for solvated **12** (in Å and °)[a]

Rh–P(1)	2.301(2)	O(1)–Rh–C(25)	89.5(2)
Rh–P(2)	2.346(2)	P(2)–Rh–C(25)	91.4(2)
Rh–O(2)	2.078(4)	O(2)–Rh–P(1)	91.6(1)
Rh–C(25)	1.793(7)	O(2)–Rh–P(2)	87.4(1)
C(25)–O(3)	1.148(8)	Rh–C(25)–O(3)	179.6(6)
Fe–Cg1	1.639(3)	∠Cp1,Cp2	2.9(5)
Fe–Cg2	1.653(4)	∠Cp1,COO	41.0(7)
C(1)–C(11)	1.494(8)	∠[Rh],Cp1	86.5(3)
C(11)–O(1)	1.238(8)	∠[Rh],COO	58.8(7)
C(11)–O(2)	1.282(7)	O(1)–C(11)–O(2)	122.2(5)
C(2)–C(12)	1.494(7)	C(2)–C(12)–P(1)	110.7(4)
P(1)–C[b]	1.800(5)–1.832(7)	C–P(1)–C[d]	103.9(3)–106.1(3)
P(2)–C[c]	1.841(6)–1.848(6)	C–P(2)–C[e]	104.4(3)–110.9(2)

[a] Definitions of the ring planes: Cp1 = C(1–5), Cp2 = C(6–10), COO = [O(1)O(2)C(11)], [Rh] = [RhP(1)P(2)O(2)C(25)]. Cg1 and Cg2 are the centroids for Cp1 and Cp2, respectively.
[b] The range of P(1)–C(12,13,19).
[c] The range of P(2)–C(31,41,51).
[d] The range of C(12)–P(1)–C(13,19) and C(13)–P(1)–C(19).
[e] The range of C(31)–P(2)–C(41,51) and C(41)–P(2)–C(51).

On going from **1** to **12**, the ligand moiety undergoes a substantial change at the diphenylphosphino group attaining a geometry similar to **9** and **10** (see above), while the Rh ← O bonding is reflected only by a slight shortening of the C(11)–O(2) and elongation of the C(1)–C(11) distances. However, the main difference can be seen in the ligand conformation: chelate formation results in rotation of the carboxyl group from the plane of the Cp1 ring by as much as ca. 41° (see Table

5 for plane definitions) and reorientation of the CH_2PPh_2 side arm (cf. the dihedral angle C(1)–C(2)–C(12)–P(1) of −79.3(7)°). Consequently, the ferrocene unit is nearly perpendicular to the coordination plane.

Phosphorus–carbon bonds ('PC_3' units) of both phosphine ligands are practically eclipsed. The cyclohexyl rings in PCy_3 adopt chair conformation with the phosphorus atom attached in equatorial positions (cf. the ring puckering parameters: C(31-26) $Q = 0.574(7)$ Å, $\varphi 1 = 2.3(7)°$; C(41-46) $Q = 0.558(8)$ Å, $\varphi 1 = 180.0(8)°$; C(51-56) $Q = 0.559(7)$ Å, $\varphi 1 = 174.9(7)°$ [33]).

3. Conclusions

Phosphinocarboxylic acid **1**, a new organometallic hybrid ligand, can be obtained by a multistep procedure in a good overall yield from the readily accessible amine **2** (56% over the three steps **2** → **4** → **5** → **1**, see Scheme 1). As shown for the case of rhodium complexes, the ligand can coordinate as a *P*-monodentate phosphine and *O*,*P*-chelating phosphinocarboxylate. A comparison of the structural data available for the ligand and its complexes indicates favourable ligand geometry, requiring no significant structural deformation upon coordination in either form.

4. Experimental

4.1. Materials and methods

Unless noted otherwise, all manipulations were carried out under argon atmosphere. *rac*-2-(*N*,*N*-dimethylaminomethyl)bromoferrocene (**2**) was prepared by metalation/bromination of (*N*,*N*-dimethylaminomethyl)ferrocene [34] as described in the literature [16]. Compounds [{(μ-Cl)RhCl(η^5-C_5Me_5)}$_2$] [35] and [Rh(acac)(CO)(PCy)$_3$][31b] were synthesized by the literature procedures. Acetic anhydride and chlorotrimethylsilane were freshly distilled under argon. Other reagents were used as received from commercial sources (Lachema, Fluka, Aldrich).

Diethyl ether and tetrahydrofuran (THF) were dried by refluxing with potassium and benzophenone until blue, and then distilled. Acetonitrile was dried with phosphorus pentoxide, distilled and stored over 4 Å molecular sieves. The dry solvent was once again distilled before use. Toluene was dried with sodium metal and distilled. Dichloromethane and chloroform were dried by standing over anhydrous potassium carbonate and distilled. Butan-2-one was dried over phosphorus pentoxide and distilled just prior to use. Solvents for workup, crystallizations and chromatography were used without purification.

NMR spectra were recorded on a Varian Unity Inova spectrometer (^{1}H, 399.95; ^{13}C, 100.58; ^{31}P, 161.90 MHz) at 25 °C. Chemical shifts (δ/ppm) are given relative to internal tetramethylsilane (^{13}C and ^{1}H) or external 85% aqueous H_3PO_4 (^{31}P). IR spectra in the range of 400–4000 cm^{-1} were measured on an FT IR Nicolet Magna 760 instrument in Nujol mulls. Mass spectra were measured either on a GS-MS Finnigan MAT INCOS 50 (GC–MS, EI mode) or on a ZAB-SEQ VG Analytical (direct inlet EI, high resolution EI and FAB spectra) spectrometers. Melting points were determined on a Kofler hot stage and are uncorrected.

4.2. Preparation of rac-(2-bromoferrocenyl)methyl acetate (3)

rac-2-(*N*,*N*-dimethylaminomethyl)bromoferrocene (**2**; 0.65 g, 2.0 mmol) was dissolved in acetic anhydride (15 mL) and the reaction flask was transferred into an oil bath heated to 100 °C. After stirring for 3 h, the mixture was cooled in an ice bath and hydrolyzed by careful addition of saturated aqueous Na_2CO_3 solution (15 mL; *caution:* exothermic, copious CO_2 evolution) and stirring for another 2.5 h, whereupon the product separated as an orange oil. The mixture was extracted with diethyl ether (3 × 15 mL), the combined organic phases were washed twice with saturated aqueous $NaHCO_3$, dried over $MgSO_4$ and evaporated under reduced pressure. The crude product was purified by column chromatography on silica gel using diethyl ether–hexane mixture (1:1) as the eluent to afford **3** as an orange oil, which solidifies to a yellow-orange solid (0.566 g, 83%).

M.p. 51–52 °C. ^{1}H NMR ($CDCl_3$): δ 2.05 (s, 3H, OC(O)*Me*), 4.16 (apparent t, $J \approx 2.6$ Hz, 1H, C_5H_3), 4.20 (s, 5H, C_5H_5), 4.30 (m, 1H, C_5H_3), 4.49 (m, 1H, C_5H_3), 4.96 (d, $^2J_{HH} = 12.2$ Hz, 1H, CH_2), 5.06 (d, $^2J_{HH} = 12.2$ Hz, 1H, CH_2). ^{13}C{^{1}H} NMR ($CDCl_3$): δ 20.91 (OC(O)C_3), 61.34 (CH_2), 67.15 (C_5H_3 *C*H), 68.41 (C_5H_3 *C*H), 70.98 (C_5H_3 *C*H), 71.16 (C_5H_5), 80.07 (C_5H_3 C_{ipso}), 80.09 (C_5H_3 C_{ipso}), 170.87 (O*C*OCH$_3$). NMR data correspond with the literature [17]. IR (Nujol, cm^{-1}): 1745 sh, 1730 vs, 1259 sh, 1240 vs, 1226 sh, 1172 w, 1106 w, 1071 w, 1026 m, 1001 m, 945 m, 916 w, 841 w, 814 m, 643 vw, 607 w, 520 w, 492 m, 456 w. GC–MS, *m*/*z* (relative abundance): 338 (29.5), 336 (31.8), 279 (2.2), 277 (3.0), 181 (10.3), 180 (100.0), 141 (7.0), 134 (20.4), 121 (28.3), 115 (10.6), 77 (6.5), 56 (13.7), 43 (10.2). HR MS: calcd. for $C_{13}H_{13}{}^{56}Fe^{79}BrO_2$ 336.9448, found 336.9439.

4.3. Preparation of rac-2-(hydroxymethyl)bromoferrocene (4)

To a methanol solution of acetate **3** (300 mg, 0.89 mmol in 25 mL) was added potassium hydroxide (2 g, 36 mmol) dissolved in water (25 mL) and the mix-

ture was heated to reflux overnight. After cooling to room temperature, the organic solvent was removed by evaporation under vacuum, and the aqueous residue extracted with diethyl ether (3 × 15 mL). The combined extracts were washed with saturated aqueous sodium chloride, dried over magnesium sulfate, and evaporated to dryness. The crude product was purified by column chromatography on silica gel, eluting with diethyl ether. A subsequent evaporation yielded alcohol **4** as a yellow orange solid. Yield: 242 mg, 92%.

M.p. 72.5–73.5 °C. ^{1}H NMR ($CDCl_3$): δ 1.64 (bs, 1H, O*H*), 4.14 (apparent t, $J \approx 2.6$ Hz, 1H, C_5H_3), 4.21 (s, 5H, C_5H_5), 4.26 (m, 1H, C_5H_3), 4.41 (d, $^2J_{HH} = 12.3$ Hz, 1H, CH_2), 4.47 (m, 1H, C_5H_3), 4.58 (d, $^2J_{HH} = 12.3$ Hz, 1H, CH_2). ^{13}C{^{1}H} NMR ($CDCl_3$): δ 59.76 (*C*H_2), 66.55 (C_5H_3 *C*H), 66.98 (C_5H_3 *C*H), 70.62 (C_5H_3 *C*H), 70.91 (*C*$_5$H$_5$), 79.39 (C_5H_3 C_{ipso}), 85.67 (C_5H_3 C_{ipso}). Analytical data are in accord with those in [17,18]. IR (Nujol, cm^{-1}): 3220 br s, 1313 m, 1252 m, 1169 w, 1104 w, 1071 w, 1031 w, 1003 s, 981 m, 947 w, 824 m, 760 br w, 695 br w, 618 w, 529 m, 488 s, 443 m. GC–MS, *m*/*z* (relative abundance): 296 (59.9), 294 (63.2), 215 (5.1), 141 (12.6), 138 (100.0), 121 (11.5), 94 (5.4), 77 (8.8), 73 (12.8), 56 (16.1). Analysis calcd. for $C_{11}H_{11}BrFeO$: 44.79% C, 3.76% H, found 44.71% C, 3.61% H.

4.4. Preparation of *4* directly from amine *2*

A solution of amine **2** (16.18 g, 50 mmol) in acetic anhydride (60 mL) was heated to 100 °C in an oil bath for 3 h while stirring and then evaporated under reduced pressure (ca. 0.5 Torr). The orange oily residue, which slowly crystallized, was immediately dissolved in methanol (50 mL) and an aqueous solution of KOH (17 g, 0.3 mol in 50 mL of water) was added. The mixture was refluxed for 20 h, cooled to room temperature, and evaporated under vacuum to remove methanol. The heterogeneous aqueous residue was extracted with diethyl ether (3 × 50 mL), the extracts were washed with water and saturated aqueous NaCl solution, and dried over $MgSO_4$ overnight. The solvent was removed under reduced pressure, the residue dissolved in hot ethyl acetate and crystallized by addition of hexane and standing at room temperature and then at −18 °C. The separated orange crystalline product was filtered off, washed with hexane and dried in air. Evaporation of the mother liquor and crystallization as above gave a second crop of the alcohol. Combined yield of **4**: 12.56 g (85%).

4.5. Preparation of rac-2-[(diphenylphosphino)methyl]-bromoferrocene (*5*)

At room temperature, neat chlorotrimethylsilane (3.15 mL, 25 mmol) was introduced to a mixture of alcohol **4** (2.95 g, 10 mmol), NaI (3.00 g, 20 mmol) and dry acetonitrile (80 mL) with stirring, whereupon the reaction mixture turned from orange to dark red and a fine precipitate formed (NaCl). After stirring for 5 min, diphenylphosphine (3.45 mL, 20 mmol) was added, causing the colour of the mixture to change to yellow. The mixture was stirred for 24 h and then quenched with saturated aqueous NaCl solution (40 mL). The mixture was diluted with diethyl ether (50 mL), the organic layer separated, washed twice with saturated aqueous NaCl solution, dried ($MgSO_4$), and then pre-adsorbed on silica gel. The solid material was transferred onto a top of a chromatographic column and eluted with hexane–diethyl ether (20:1). Unreacted phosphine is eluted first followed by a yellow band of the product, which was collected and evaporated to give **5** as an orange oil, which solidified at 4 °C. Yield: 4.17 g (90%).

M.p. 55–56 °C. ^{1}H NMR ($CDCl_3$): δ 3.20 (d, 1H, $^2J_{HH} = 14.2$ Hz CH_2), 3.30 (d, 1H, $^2J_{HH} = 14.2$ Hz CH_2), 3.77 (m, 1H, C_5H_3), 3.94 (apparent t, $J \approx 2.6$ Hz, 1H, C_5H_3), 4.13 (s, 5H, C_5H_5), 4.36 (m, 1H, C_5H_3), 7.31–7.48 (m, 10H, P*Ph*$_2$). ^{13}C{^{1}H} NMR ($CDCl_3$): δ 28.54 (d, $^1J_{PC} = 16$ Hz, *C*H_2), 65.61 (C_5H_3 *C*H), 67.16 (d, $^3J_{PC} = 6$ Hz, C_5H_3 *C*H), 69.38 (C_5 H_3 *C*H), 71.33 (*C*$_5$H$_5$), 80.51 (d, $^3J_{PC} = 3$ Hz, C_5H_3 *C*–Br), 83.36 (d, $^2J_{PC} = 16$ Hz, C_5H_3 *C*–CH_2), 128.32 (d, $^3J_{PC} = 3$ Hz, PPh_2 C_m), 128.39 (d, $^3J_{PC} = 4$ Hz, PPh_2 *C*H_m), 128.41 (PPh_2 *C*H_p), 128.96 (PPh_2 *C*H_p), 132.35 (d, $^2J_{PC} = 18$ Hz, PPh_2 *C*H_o), 133.46 (d, $^2J_{PC} = 20$ Hz, PPh_2 *C*H_o), 138.12, 138.47 (2× d, $^1J_{PC} = 15$ Hz, PPh_2 C_{ipso}). ^{31}P{^{1}H} NMR ($CDCl_3$): δ −13.7 (s). MS (direct inlet), *m*/*z* (relative abundance): 465 (10.4), 464 (37.9), 463 (11.2), 462 (40.9), 306 (5.0), 280 (13.8), 279 (94.0), 278 (17.9), 277 (100.0), 197 (23.5), 183 (39.5), 141 (37.0), 121 (15.9), 115 (15.6), 56 (17.3). HR MS: calcd. for $C_{23}H_{20}{}^{56}Fe^{79}BrOP$ (phosphine oxide) 477.9785, found 477.9791.

4.6. Synthesis of rac-2-[(diphenylphosphino)methyl]-ferrocenecarboxylic acid (*1*)

A solution of phosphine **5** (3.61 g, 7.8 mmol) in THF (60 mL) cooled to −78 °C (ethanol/CO_2) was treated with butyl lithium (3.9 mL, 2.5 M in hexanes, 9.8 mmol). After stirring for 1 h at −78 °C, the reaction solution was poured onto a large excess of finely crushed solid CO_2 (ca. 50 g) and allowed to stand overnight at room temperature. Then, the mixture was diluted with dichloromethane (20 mL), washed with saturated aqueous NaCl solution (2× 30 mL). The organic phase was dried over $MgSO_4$ and evaporated under vacuum. The residue was purified by chromatography on silica gel with dichloromethane–methanol (10:1). Some [(diphenylphosphino) methyl]ferrocene was eluted first (ca. 0.49 g, identified by NMR spectroscopy [23]), followed by a second major band of acid **1**, which after evaporation afforded the acid as an orange solid. Yield: 2.44 g (73%).

M.p. 172–173 °C. ^{1}H NMR ($CDCl_3$): δ 3.34 (dd, $^2J_{HH} = 13.7$ Hz, $^2J_{PH} \approx 1.3$ Hz, 1H, CH_2), 3.90 (d, $^2J_{HH} = 13.7$ Hz, 1H, CH_2), 4.06 (m, 1H, C_5H_3), 4.18 (s, 5H, C_5H_5), 4.25 (apparent t, $J \approx 2.6$ Hz, 1H, C_5H_3), 4.77 (m, 1H, C_5H_3), 7.29–7.48 (m, 10H, PPh_2). ^{13}C{^{1}H} NMR ($CDCl_3$): δ 28.57 (d, $^1J_{PC} = 15$ Hz, CH_2), 67.56 (d, $^3J_{PC} = 3$ Hz, C_5H_3 C–CO_2H), 70.00 (C_5H_3 CH), 70.77 (C_5H_3 CH), 70.85 (C_5H_5), 73.71 (d, $^3J_{PC} = 5$ Hz, C_5H_3 CH), 87.92 (d, $^2J_{PC} = 16$ Hz, C_5H_3 C–CH_2), 128.23, 128.27 (2× PPh_2 CH_m), 128.34, 128.91 (2× PPh_2 CH_p); 132.29 (d, $^2J_{PC} = 18$ Hz, PPh_2 CH_o), 133.66 (d, $^2J_{PC} = 20$ Hz, PPh_2 CH_o), 138.22, 138.73 (2× d, $^1J_{PC} = 15$ Hz, PPh_2 CH_{ipso}); 178.67 (C_2H). ^{31}P{^{1}H} NMR ($CDCl_3$): δ −10.1 (s). IR (Nujol, cm^{-1}): 1661 s, 1409 w, 1347 w, 1306 sh, 1289 s, 1229 m, 1173 w, 1155 w, 1113 w, 1104 m, 1072 w, 1038 w, 997 w, 934 br w, 863 w, 843 w, 827 w, 815 w, 783 w, 763 w, 752 m, 741 s, 701 m, 691 m, 626 w, 559 w, 516 m, 506 m, 494 w, 483 m, 471 m. MS (direct inlet), *m*/*z* (relative abundance): 429 (15.5), 428 (51.0), 306 (14.2), 257 (5.7), 244 (30.4), 243 (100.0), 199 (16.2), 186 (14.2), 183 (18.9), 121 (8.8), 108 (24.5), 105 (53.0), 57 (19.6). HR MS: calcd. for $C_{24}H_{21}{}^{56}FeO_2P$ 428.0629, found 428.0652. Analysis calcd. for $C_{24}H_{21}FeO_2P$: 67.31% C, 4.94% H, found 66.79% C, 4.86% H.

4.7. Preparation of rac-2-[(diphenylphosphoryl)methyl]-ferrocenecarboxylic acid (6)

In air, hydrogen peroxide (0.5 mL 30%, 4 mmol) was added dropwise to a stirred solution of acid **1** (160 mg, 0.37 mmol) in acetone (15 mL) with cooling in an ice bath. After the addition had been completed, the cooling bath was removed and stirring was continued at room temperature for 15 min (the conversion was complete in this time according to TLC analysis). Then, acetone was removed under reduced pressure, the residue diluted with water (20 mL) and extracted with dichloromethane (3 × 15 mL). Combined extracts were washed with saturated aqueous NaCl solution (20 mL), dried shortly over $MgSO_4$, and evaporated under vacuum. The residue was purified by column chromatography on silica gel eluting with dichloromethane–methanol (10:1) to yield **6** as a brown solid after evaporation. Yield: 84 mg (51%; a considerable amount of a dark material remains adsorbed at the top of the chromatographic column).

M.p. 120–122 °C (dec.). ^{1}H NMR ($CDCl_3$): δ 3.57 (virtual t, $^2J_{HH} \approx {}^2J_{PH} \approx 14.8$ Hz, 1H, CH_2), 4.17 (s, 5H, C_5H_5), 4.30 (apparent t, $J \approx 2.6$ Hz, 1H, C_5H_3), 4.42 (dd, $^2J_{HH} = 15.1$ Hz, $^2J_{PH} = 10.6$ Hz, 1H, CH_2), 4.46 (m, 1H, C_5H_3), 4.75 (m, 1H, C_5H_3), 7.34–7.80 (m, 10H, PPh_2). ^{13}C{^{1}H} NMR ($CDCl_3$): δ 31.13 (d, $^1J_{PC} = 67$ Hz, CH_2), 70.32 (C_5H_3 CH), 71.03 (C_5H_5), 71.72 (C_5H_3 CH), 73.66 (d, $^3J_{PC} = 2$ Hz, C_5H_3 CH), 79.92 (d, $^2J_{PC} = 4$ Hz, C_5H_3 C–CH_2), 128.34, 128.55 (2× d, $^3J_{PC} = 12$ Hz, PPh_2 CH_m); 130.86 (d, $^1J_{PC} = 34$ Hz, PPh_2 CH_{ipso}), 131.17, 131.27 (2× d, $^2J_{PC} = 7$ Hz, PPh_2 CH_o); 131.85 (d, $^1J_{PC} = 34$ Hz, PPh_2 CH_{ipso}), 131.89, 132.00 (2× d, $^4J_{PC} = 3$ Hz, PPh_2 CH_p); 175.22 (CO_2H), signal due to C(C_5H_3)–CO_2H was not found. ^{31}P{^{1}H} NMR ($CDCl_3$): δ 32.2 (s). IR (Nujol, cm^{-1}): 1689 s, 1591 w, 1281 m, 1213 m, 1171 s, 1120 s, 1099 s, 1074 m, 1036 w, 1001 m, 818 m, 785 w, 741 s, 694 s, 525 m, 507 s, 434 w. MS (direct inlet), *m*/*z* (relative abundance): 445 (29.8), 444 (100.0), 400 (4.9), 380 (18.9), 379 (81.8), 336 (10.5), 335 (46.2), 333 (11.9), 322 (14.4), 257 (7.3), 201 (11.9), 183 (7.4), 121 (14.0), 105 (51.1), 77 (24.8), 56 (15.5). HR MS: calcd. for $C_{24}H_{21}{}^{56}FeO_3P$ 444.05778, found 444.0595.

4.8. Preparation of rac-2-[(diphenylthiophosphoryl)methyl]ferrocenecarboxylic acid (7)

A solution of acid **1** (170 mg, 0.40 mmol) and sulfur (14 mg, 0.44 mmol) in toluene (20 mL) was heated at reflux for 1 h. After cooling to room temperature, the solution was evaporated to ca. 5 mL and allowed to crystallize at −18 °C overnight. The orange microcrystalline solid was filtered off and dried in air. Yield: 156 mg (85%).

M.p. dec. above 135 °C. ^{1}H NMR ($CDCl_3$): δ 3.59 (virtual t, $^2J_{HH} \approx {}^2J_{PH} \approx 14.3$ Hz, 1H, CH_2), 4.19 (s, 5H, C_5H_5), 4.41 (apparent t, $J = 2.7$ Hz, 1H, C_5H_3), 4.69 (m, 1H, C_5H_3), 4.77 (dd, $^2J_{HH} \approx {}^2J_{PH} \approx 12$ Hz, 1H, CH_2), 4.77 (m, 1H, C_5H_3), 7.16–7.98 (m, 10H, PPh_2). ^{13}C{^{1}H} NMR ($CDCl_3$): δ 34.78 (d, $^1J_{PC} = 49$ Hz, CH_2), 67.63 (d, $^3J_{PC} \approx 1$ Hz, C_5H_3 C–CO_2H), 70.74 (C_5H_3 CH), 70.94 (C_5H_3 CH), 71.09 (C_5H_5), 74.66 (d, $^3J_{PC} \approx 2$ Hz, C_5H_3 CH), 81.73 (d, $^2J_{PC} \approx 2$ Hz, C_5H_3 C–CH_2), 127.96, 128.55 (2× d, $^3J_{PC} = 12$ Hz, PPh_2 CH_m); 128.61 (d, $^1J_{PC} = 81$ Hz, PPh_2 C_{ipso}), 131.27, 131.61 (2× d, $^4J_{PC} = 3$ Hz, PPh_2 CH_p); 131.70, 131.80 (2× d, $^2J_{PC} = 6$ Hz, PPh_2 CH_o); 131.81 (d, $^1J_{PC} = 153$ Hz, PPh_2 C_{ipso}), 177.47 (C_2H). ^{31}P{^{1}H} NMR ($CDCl_3$): δ 42.4 (s). IR (Nujol, cm^{-1}): 1678 s, 1295 s, 1241 w, 1222 w, 1105 m, 1078 w, 998 m, 866 m, 840 m, 814 w, 742 m, 732 m, 707 m, 690 m, 643 w, 601 w, 499 w, 488 w. MS (direct inlet), *m*/*z* (relative abundance): 461 (24.7), 460 (83.2), 428 (8.2), 416 (16.7), 396 (11.7), 395 (48.2), 351 (17.2), 338 (13.7), 273 (10.3), 244 (11.5), 243 (55.9), 217 (9.6), 199 (15.3), 185 (10.7), 183 (16.2), 149 (12.8), 121 (8.8), 105 (53.0), 92 (80.1), 91 (100.0), 69 (25.0), 56 (11.5). HR MS: calcd. for $C_{24}H_{21}{}^{56}FeO_2PS$ 460.0349, found 460.0334.

4.9. Preparation of methyl rac-2-[(diphenylphosphino)methyl]ferrocenecarboxylate (8)

A solution of diazomethane in diethyl ether (prepared from 5 mmol of *N*-methyl-*N*-nitroso-*p*-toluenesulfonamide) was added to a solution of acid **1** (0.400 g, 0.93 mmol) in THF (10 mL). The mixture was stirred

at room temperature for 30 min and then evaporated under vacuum. The residue was purified by column chromatography (silica gel, diethyl ether). Evaporation of a single band gave methyl ester **8** as an oil, which solidified upon standing at 4 °C. Yield: 0.404 g (98%). According to NMR spectra, the product is contaminated with trace amount of the respective phosphine oxide, which forms slowly in the air.

M.p. 58–60 °C. ^{1}H NMR ($CDCl_3$): δ 3.31 (dd, $^2J_{HH} = 13.7$, $^2J_{PH} = 1.5$ Hz, 1H, CH_2), 3.74 (s, 3H, CO_2Me), 3.89 (d, $^2J_{HH} = 13.7$, 1H, CH_2), 4.00 (m, 1H, C_5H_3), 4.11 (s, 5H, C_5H_5), 4.17 (apparent t, $J \approx 2.7$ Hz, 1H, C_5H_3), 4.68 (m, 1H, C_5H_3), 7.25–7.46 (m, 10H, PPh_2). ^{13}C{^{1}H} NMR ($CDCl_3$): δ 28.98 (d, $^1J_{PC} = 15$ Hz, CH_2), 51.31 (CO_2Me), 68.88 (d, $^3J_{PC} = 2$ Hz, C_5H_3 C–CO_2Me), 69.30 (C_5H_3 CH), 70.12 (C_5H_3 CH), 70.47 (C_5H_5), 72.99 (d, $^3J_{PC} = 5$ Hz, C_5H_3 CH), 87.46 (d, $^2J_{PC} = 16$ Hz, C_5H_3 C–CH_2), 128.16, 128.25 (2× d, $^3J_{PC} = 3$ Hz, PPh_2 CH_m); 128.38, 128.91 (2× PPh_2 CH_p); 132.24 (d, $^2J_{PC} = 18$ Hz, PPh_2CH_o), 133.68 (d, $^2J_{PC} = 20$ Hz, PPh_2 CH_o), 138.17, 138.93 (2× d, $^1J_{PC} = 15$ Hz, PPh_2 C_{ipso}); 172.58 (CO_2Me). ^{31}P{^{1}H} NMR ($CDCl_3$): δ −10.1 (s). IR (Nujol, cm^{-1}): 1704 s, 1403 w, 1366 sh, 1287 s, 1216 m, 1101 m, 1075–1069 w, 1015 w, 997 w, 933 w, 862 w, 827 w, 775 w, 757 w, 742 m, 695 m, 519 w, 507 w, 494 w, 472 w, 464 w, 432 w. MS (direct inlet), *m/z* (relative abundance): 443 (12.6), 442 (40.9), 306 (9.4), 258 (17.9), 257 (100.0), 183 (7.8), 121 (4.7), 105 (43.9), 56 (3.4). HR MS: calcd. for $C_{25}H_{23}{}^{56}FeO_2P$ 442.0785, found 442.0764.

4.10. Preparation of dichloro-{rac-2-[(diphenylphosphino-κP)methyl]ferrocenecarboxylic acid}-(η^5-pentamethylcyclopentadienyl)rhodium(III) (**9**)

A solution of [{(μ-Cl)RhCl(η^5-C_5Me_5)}$_2$] (62 mg, 0.10 mmol) in dichloromethane (10 mL) was added to a solution of carboxyphosphine **1** (86 mg, 0.20 mmol) in the same solvent (10 mL). The mixture was stirred at room temperature for 1 h and evaporated under vacuum. The residue was redissolved in dichloromethane (3 mL), the solution was layered with hexane and allowed to crystallized by diffusion at room temperature. Orange red needles of complex **9**, which separated after several days, were filtered off, washed with hexane and dried in air. Yield: 141 mg (96%). (*Note:* in repeated syntheses, dichloromethane was replaced with chloroform and the product was precipitated with excess hexane without lowering the yield or product purity).

M.p. dec. above 240 °C. ^{1}H NMR ($CDCl_3$): δ 1.36 (d, $^3J_{RhH} = 3.4$ Hz, 15H, C_5Me_5), 3.87 (m, 1H, C_5H_3), 4.05 (apparent t, $J \approx 2.7$ Hz, 1H, C_5H_3), 4.13 (s, 5H, C_5H_5), 4.25 (dd, $^2J_{HH} = 15.3$, $^2J_{PH} = 9$ Hz, 1H, CH_2), 4.54 (m, 1H, C_5H_3), 4.56 (dd, $^2J_{HH} = 15.3$, $^2J_{PH} = 7$ Hz, 1H, CH_2), 7.33–7.88 (m, 10H, PPh_2). ^{13}C{^{1}H} NMR ($CDCl_3$): δ 8.64 (d, $^2J_{RhC} \approx 1$ Hz, C_5Me_5), 28.95 (d, $^1J_{PC} = 21$ Hz, C_2), 68.70 (C_5H_3 C–CO_2H), 70.09 (C_5H_3 CH), 70.28 (C_5H_3 CH), 70.99 (C_5H_5), 74.78 (C_5H_3 CH), 85.05 (d, $^2J_{PC} = 10$ Hz, C_5H_3 C–CH_2), 98.51 (dd, $^1J_{RhC} = 7$ Hz, $^2J_{PC} = 3$ Hz, C_5Me$_5$), 127.20 (d, $^1J_{PC} = 43$ Hz, PPh_2 C_{ipso}), 127.64, 127.68 (2× d, $^3J_{PC} = 10$ Hz, PPh_2 CH_m); 129.35 (d, $^1J_{PC} = 41$ Hz, PPh_2 C_{ipso}), 130.42, 130.90 (2× d, $^4J_{PC} = 2$ Hz, PPh_2 CH_p); 134.17, 135.26 (2× d, $^2J_{PC} = 9$ Hz, PPh_2 CH_o); 176.05 (CO_2H). ^{31}P{^{1}H} NMR ($CDCl_3$): δ 35.1 (d, $^1J_{RhP} = 141$ Hz). IR (Nujol, cm^{-1}): 1677 s, 1635 sh, 1399 w, 1298–1289 m, 1250 w, 1236 w, 1215 w, 1183 w, 1157 w, 1107 w, 1098 m, 1071 w, 1026 w, 1000 w, 861 w, 825 m, 813 w, 744 s, 725 m, 696 m, 661 w, 615 w, 562 w, 521 w, 505 m, 487 m, 447 m. FAB$^+$ (thioglycerol–glycerol), *m/z*: 701 ([M − Cl]$^+$), 666 ([M − 2Cl]$^+$); M$^+$ not observed. HR MS (FAB): calcd. for $C_{34}H_{36}{}^{35}Cl^{56}FeO_2PRh$ 701.0546, found 701.0539; calcd. for $C_{34}H_{36}{}^{56}FeO_2PRh$ 666.0857, found 666.0880.

4.11. Preparation of dichloro-{methyl rac-2-[(diphenylphosphino-κP)methyl]ferrocenecarboxylate}-(η^5-pentamethylcyclopentadienyl)rhodium(III) (**10**)

A solution of [{(η-Cl)RhCl(η^5-C_5Me_5)}$_2$] (62 mg, 0.10 mg) in chloroform (10 mL) was mixed with a solution of phosphinoester **8** (89 mg, 0.20 mmol) in the same solvent (10 mL). The reaction mixture was stirred at room temperature for 1 h and then evaporated under reduced pressure. The solid residue was dissolved in chloroform (3 mL), the solution was filtered and crystallized by addition of hexane and standing overnight at −18 °C to give **10** as a dark red crystalline solid, which was filtered off and dried in air. Yield: 106 mg (71%).

M.p. dec. above 120 °C. ^{1}H NMR ($CDCl_3$): δ 1.33 (d, $^3J_{RhH} = 3.5$ Hz, 15H, C_5Me_5), 3.39 (s, 3H, CO_2Me), 3.78 (m, 1H, C_5H_3), 4.05 (apparent t, $J \approx 2.6$ Hz, 1H, C_5H_3), 4.07 (s, 5H, C_5H_5), 4.21 (dd, $^2J_{HH} = 15.5$, $^2J_{PH} = 8.3$ Hz, 1H, CH_2), 4.46 (dd, $^2J_{HH} = 15.5$, $^2J_{PH} = 7.0$ Hz, 1H, CH_2), 4.52 (m, 1H, C_5H_3), 7.22–7.94 (m, 10H, PPh_2). ^{13}C{^{1}H} NMR ($CDCl_3$): δ 8.59 (d, $^2J_{RhC} \approx 1$ Hz, C_5Me_5), 29.07 (d, $^1J_{PC} = 21$ Hz, CH_2), 50.98 (CO_2Me), 69.70 (C_5H_3, CH), 69.83 (C_5H_3, CH), 70.53 (C_5H_5), 71.61 (C–COOH, C_5H_3), 73.01 (C_5H_3, CH), 83.82 (d, $^2J_{PC} = 10$ Hz, C–$CH_2C_5H_3$), 98.50 (dd, $^1J_{RhC} = 7$ Hz, $^2J_{PC} = 3$ Hz, C_5Me$_5$), 125.40 (d, $^1J_{PC} = 42$ Hz, C_{ipso} PPh_2), 127.14, 127.93 (2× d, $^3J_{PC} = 10$ Hz, C_m PPh_2); 130.32 (d, $^4J_{PC} = 2$ Hz, C_p PPh_2), 131.00 (d, $^1J_{PC} = 40$ Hz, C_{ipso} PPh_2), 131.24 (d, $^4J_{PC} = 2$ Hz, C_p PPh_2), 132.76 (d, $^2J_{PC} = 7$ Hz, CH_o PPh_2), 136.33 (d, $^2J_{PC} = 10$ Hz, CH_o PPh_2), 171.69 (COOMe). ^{31}P{^{1}H} NMR ($CDCl_3$): δ 35.0 (d, $^1J_{RhP} = 142$ Hz). IR (Nujol, cm^{-1}): 1712 m, 1687 s, 1506 w, 1408 w, 1296 s, 1248 w, 1233 m, 1213 w, 1194 w, 1174 m, 1159 w, 1122 w, 1107 w, 1099 m, 1080 w, 1015 m, 861 w, 846 w, 836 w, 824 w, 777 w, 752 sh,

744 s, 704 sh, 697 m, 660 w, 612 w, 522 w, 504 m, 489 m, 445 m. FAB^+ (thioglycerol–glycerol), *m/z*: 751 ($[M - Cl]^+$), 680 ($[M - 2Cl]^+$); M^+ not observed. HR MS (FAB): calcd. for $C_{35}H_{38}{}^{35}Cl^{56}FeO_2PRh$ 715.0702, found 715.0689; calcd. for $C_{35}H_{38}{}^{56}FeO_2PRh$ 680.1014, found 680.0997.

4.12. Attempted preparation of O,P-chelate complexes by deprotonation of 9

Butyl lithium (0.1 mL 2.5 M in hexanes, 0.25 mmol) was added to a solution of complex **9** (148 mg, 0.20 mmol) in THF (10 mL) at room temperature. After stirring for 24 h, the volatiles were removed under vacuum and the residue was subjected to column chromatography on silica gel using dichloromethane–methanol (10:1) as the eluent. NMR analysis of the fractions collected indicated the presence of unchanged **9** and a two compounds in a ratio of ca. 10:1, which were tentatively assigned to diastereoisomers of chloro-{*rac*-2-[(diphenylphosphino-κ*P*)methyl]ferrocenecarboxylate-κ*O*}-(η^5-pentamethylcyclopentadienyl)rhodium(III) (**11**). Subsequent attempts to purify the obtained material by crystallization or chromatography gave either intractable mixtures or the starting complex **9**.

NMR data for the more abundant new component: ^{1}H NMR ($CDCl_3$): δ 1.56 (d, $^3J_{RhH} = 3.4$ Hz, 15H, C_5Me_5), 3.02 (dd, $^2J_{PH} = 16.7$, $^2J_{HH} = 12.6$ Hz, 1H, CH_2), 3.37 (m, 1H, C_5H_3), 3.83 (apparent t, $J \approx 2.6$ Hz, 1H, C_5H_3), 4.12 (s, 5H, C_5H_5), 4.42 (dd, $^2J_{HH} = 12.5$, $^2J_{PH} = 9.3$ Hz, 1H, CH_2), 4.78 (m, 1H, C_5H_3), 6.98–7.65 (m, 10H, PPh_2). $^{31}P\{^1H\}$ NMR ($CDCl_3$): δ 41.0 (d, $^1J_{RhP} = 149$ Hz). The minor component: $^{31}P\{^1H\}$ NMR ($CDCl_3$): δ 41.4 (d, $^1J_{RhP} = 151$ Hz).

4.13. Synthesis of [SP-4-2]-carbonyl-[rac-2-{(diphenylphosphino)methyl}ferrocenecarboxylato-κ^{2}O,P]-tricyclohexylphosphinerhodium(I) (12)

To a warm solution [Rh(acac)(CO)(PCy_3)] (51 mg, 0.10 mmol) in butan-2-one (3 mL) was added acid **1** dissolved in the same solvent (47 mg, 0.11 mmol in 3 mL) and the mixture was heated at reflux for 5 min. The reaction solution was cooled to room temperature and the volatiles were removed under vacuum. The residue was immediately dissolved in methanol (3 mL; the product starts to crystallize instantly) and the solution was allowed to crystallize overnight at −18 °C. The separated yellow microcrystalline product was filtered off, washed with methanol and diethyl ether and dried in air. Yield: 71 mg, 85%; characterized as the solvate **12** · $0.7H_2O$.

M.p. 149–151 °C (dec.). ^{1}H NMR ($CDCl_3$): δ 1.16–2.34 (m, 33H, PCy_3), 3.22 (ddd, $J = 13.6$, 13.5, 5.1 Hz, 1H, CH_2PPh_2), 3.44 (m, 1H, C_5H_3), 3.49 (br s, 1.4H, H_2O), 3.91 (apparent t, $J \approx 2.5$ Hz, 1H, C_5H_3), 3.96 (dd, $J = 12.8$, 5.2 Hz, 1H, CH_2PPh_2), 4.13 (s, 5H, C_5H_5), 4.69 (m, 1H, C_5H_3), 7.29–7.82 (m, 10H, PPh_2). $^3C\{^1H\}$ NMR ($CDCl_3$): δ 26.60 (s, PCy_3 γ-CH_2), 27.57 (d, $^3J_{PC} = 10$ Hz, PCy_3 β-CH_2), 29.72 (dd, $^1J_{PC} = 18$ Hz, $^2J_{RhC} \approx 2$ Hz, CH_2PPh_2), 30.23 (d, $^2J_{PC} = 38$ Hz, PCy_3 α-CH_2), 33.45 (d, $^1J_{PC} = 18$ Hz, PCy_3 *C*H), 66.37 (C_5H_3 *C*H), 69.80 (d, $^3J_{PC} = 2$ Hz, C_5H_3 *C*H), 70.59 (C_5H_5), 72.01 (C_5H_3 *C*H), 77.44 (d, $^3J_{PC} = 7$ Hz, C_5H_3 *C*–COOH), 85.55 (d, $^2J_{PC} = 2$ Hz, C_5H_3 *C*–CH_2), 127.97, 128.78 (2× d, $^1J_{PC} = 9$ Hz, PPh_2 C_m); 130.30, 130.34 (2× d, $^4J_{PC} = 2$ Hz, PPh_2 CH_p); 132.58, 133.72 (2× d, $^3J_{PC} = 11$ Hz, PPh_2 CH_m); 175.28 (*C*=O), 190.11 (dt, $^1J_{RhC} = 72$ Hz, $^2J_{PC} = 16$ Hz, *C*≡O); the C_{ipso} (PPh_2) signals are obscured by other phenyl resonances. $^{31}P\{^1H\}$ NMR ($CDCl_3$): δ 32.8 (dd, $^1J_{RhP} = 128$ Hz, $^2J_{PP} = 322$ Hz, PPh_2), 40.9 (dd, $^1{}_{RhP} = 126$ Hz, $^2J_{PP} = 322$ Hz, PCy_3). IR (Nujol, cm^{-1}): 1956 vs, 1624 w, 1603 s, 1582 m, 1564 w, 1398 vw, 1351 sh, 1331 m, 1314 w, 1301 w, 1246 w, 1176 w, 1101 w, 1043 w, 1028 vw, 1000 w, 852 vw, 830 w, 783 w, 745–733 m str, 693 w, 591 w, 557 vw, 514 vw, 488 w, 466 vw. Analysis calcd. for $C_{43}H_{53}FeO_3P_2Rh \cdot H_2O$: 60.29% C, 6.47% H; found 60.25% C, 6.43% H.

4.14. X-ray crystallography

Crystals suitable for diffraction measurements have been obtained by crystallization from hot hexane (**4**: yellow plate, $0.06 \times 0.13 \times 0.25$ mm^3), ca. 50% aqueous acetic acid (**1**: rusty orange plate, $0.05 \times 0.13 \times 0.25$ mm^3; **9**: red prism, $0.10 \times 0.15 \times 0.28$ mm^3), and methanol (solvated **12**: tiny yellow needle: $0.03 \times 0.05 \times 0.30$ mm^3), or by liquid-phase diffusion from chloroform–hexane (**6**: rusty orange block, $0.23 \times 0.25 \times 0.30$ mm^3), dichloromethane–hexane (**7**: orange plate, $0.13 \times 0.28 \times 0.50$ mm^3), and ethyl acetate–hexane (**10**: red prism, $0.13 \times 0.18 \times 0.23$ mm^3). Full-set diffraction data ($\pm h \pm k \pm l$, $\theta \leqslant 27.5°$) were collected on a Nonius Kappa CCD diffractometer equipped with a Cryostream Cooler (Oxford Cryosystems) using graphite monochromatized Mo Kα radiation ($\lambda = 0.71073$ Å) and analyzed with HKL program package [36]. The data for **2**, solvated **10** and **11** were corrected for absorption by a numerical method based on intensity variation for multiply measured diffractions as incorporated in the diffractometer software (SORTAV routine [37]). The structures were solved by direct methods (SIR97 [38]) and refined by weighted full-matrix least-squares procedure on F^2 (SHELXL97 [39]).

All non-hydrogen atoms were refined with anisotropic thermal motion parameters. Carboxylic hydrogen atoms in **1** and **6** as well as the hydroxyl hydrogen atoms in **4** were identified on difference Fourier maps and isotropically refined. The position of acidic hydrogen in **7** was located similarly and refined with $U_{iso}(H) = 1.2U_{eq}(O)$. Carboxylic hydrogen atom in **9** was identified on a difference Fourier map and subsequently refined

Table 6
Crystallographic data and data collection and structure refinement parameters for **4**, **1**, **6** · $CHCl_3$, **7** · 1/2CH_2Cl_2, **9**, **10**, and **12**

Compound	**4**	**1**	**6** · $CHCl_3$	**7** · 1/2CH_2Cl_2	**9**	**10**	**12**
Formula	$C_{11}H_{11}BrFeO$	$C_{24}H_{21}FeO_2P$	$C_{25}H_{22}Cl_3FeO_3P$[f]	$C_{24.5}H_{22}ClFeO_2PS$[g]	$C_{34}H_{36}Cl_2FeO_{3.5}PRh$[h]	$C_{35}H_{38}Cl_2FeO_2PRh$	$C_{43}H_{53}FeO_{3.7}P_2Rh$[j]
M (g mol^{-1})	294.96	428.23	563.60	502.75	761.26	751.28	849.75
Crystal system	Monoclinic	Monoclinic	Triclinic	Triclinic	Monoclinic	Monoclinic	Orthorhombic
Space group	$C2/c$ (no. 15)	$P2_1/c$ (no. 14)	$P\bar{1}$ (no. 2)	$P\bar{1}$ (no. 2)	$P2_1/n$ (no. 14)	$P2_1/n$ (no. 14)	$P2_12_12_1$ (no. 19)
a (Å)	26.0392(5)	8.7357(3)	10.0374(3)	7.0924(2)	10.6862(1)	9.1402(1)	11.3304(2)
b (Å)	6.7871(1)	19.3632(6)	10.8070(3)	12.6061(3)	10.2992(1)	32.6789(5)	14.2815(3)
c (Å)	25.1973(5)	11.9639(3)	11.6368(3)	14.2396(4)	30.7045(4)	11.6107(2)	26.1049(5)
α (°)			77.978(2)	106.050(1)			
β (°)	104.184(1)	102.133(2)	80.357(2)	93.817(1)	95.4566(8)	111.8426(8)	
γ (°)			83.161(2)	99.914(2)			
Z	16	4	2	2	4	4	4
V (Å^3)	4317.4(1)	1978.5(1)	1212.52(6)	1196.43(6)	3364.00(6)	3219.05(8)	4224.2(1)
D_{calc} (g mL^{-1})	1.815	1.438	1.544	1.396	1.503	1.550	1.336
T (K)	150(2)	150(2)	150(2)	150(2)	150(2)	150(2)	150(2)
μ (Mo Kα) (mm^{-1})	5.061	1.438	1.045	0.914	1.162	1.210	0.847
T[a]	0.591–0.731	–[e]	–[e]	0.591–0.731	0.798–0.894	0.644–0.935	–[e]
Collected diffrations, R_{int} (%)[b]	30,594, 4.5	36,709, 7.3	18,715, 2.6	21,465, 3.0	47,798, 4.6	40,462, 5.3	58,572, 11.9
Unique/observed[c] diffractions	4937/3981	4545/2758	5549/4877	5493/4716	7691/6442	7359/5637	7442/5597
R (observed data) (%)[d]	3.29	4.90	3.36	4.21	3.96	3.49	4.83
R, wR (all data) (%)[d]	4.80, 7.95	10.24, 12.14	4.04, 8.41	5.12, 12.1	5.10, 10.4	5.79, 7.28	8.52, 11.1
$\Delta\rho$ (e Å^{-3})	0.52, 0.68	0.42, −0.42	0.55, −0.57	0.83, −0.83[i]	1.34, −0.74[i]	0.63, −0.52	0.57, −0.41

[a] The range of transmission coefficients.
[b] $R_{int} = \sum |F_o^2 - F_o^2(\text{mean})| / \sum F_o^2$, where F_o^2(mean) is the average intensity for symmetry equivalent diffractions.
[c] Diffractions with $I_0 > 2\sigma(I_0)$.
[d] $R = \sum \|F_o\| - \|F_c\| / \sum F_o\|$, $wR = [\sum \{w(F_o^2 - F_c^2)^2\} / \sum w(F_o^2)^2]^{1/2}$.
[e] Not corrected.
[f] $C_{24}H_{21}FeO_3P \cdot CHCl_3$.
[g] $C_{24}H_{21}FeO_2PS \cdot 1/2CH_2Cl_2$.
[h] $C_{34}H_{36}Cl_2FeO_2PRh \cdot O_{1.5}$.
[i] Residuals in the space accommodating the disordered solvate molecules.
[j] $C_{43}H_{53}FeO_3P_2Rh \cdot O_{0.7}$.

using a riding model and assigned $U_{iso}(H) = 1.2U_{eq}(O)$. Other hydrogen atoms were included in the calculated positions and refined using the riding model [C–H bond lengths: 0.96 (methyl), 0.97 (methylene), 0.98 (methine), and 0.93 (aromatic); $U_{iso}(H) = 1.5U_{eq}(C)$ (methyl) or $U_{iso}(H) = 1.2U_{eq}(C)$ (all other)].

The structure of **7** contains molecules of solvating dichloromethane. The solvate molecules are extensively disordered in channels defined by the non-polar phenyl and ferrocene moieties, running parallel to the crystallographic *a*-axis. The disordered solvent molecules were modelled over two independent positions with fractional occupancies 0.40 and 0.10, thus, giving one dichloromethane molecule per the unit cell.

The crystals of **9** obtained from aqueous acetic acid accommodate water molecules in the space close to the carboxyl groups of the ligands. The water molecules, which seem to occupy various positions with fractional occupancies (though in the usual hydrogen bond distances), were included in the refined model only as oxygen atoms with partial occupancies (0.8, 0.5, and 0.2; the first two anisotropically and the least populated with an isotropic thermal motion parameter).

The solvate molecules in hydrate **12** · $0.7H_2O$ were refined similarly (occupancies 0.3, 0.3, and 0.2; all with isotropic thermal motion parameters). The crystals suffered from racemic twinning. The refinement revealed practically identical contributions from the enantiomeric forms (0.488:0.512).

Selected crystallographic data are given in Table 6. The geometric data presented and the molecular drawings were obtained with a recent version of PLATON program [40].

5. Supplementary material

Crystallographic data excluding structure factors have been deposited with the Cambridge Crystallographic Data Centre. Copies of the data can be obtained upon application to The Director, CCDC, 12 Union Road, Cambridge, CB2 1EZ, UK (fax: +44 1223 336408; e-mail: deposit@ccdc.cam.ac.uk). CCDC reference numbers: CCDC-266155 (**4**), -266156 (**1**), -266157 (**6** · $CHCl_3$), -266158 (**7** · $1/2CH_2Cl_2$), -266159 (**9** hydrate), -266160 (**10**), and -266161 (**12** hydrate).

Acknowledgement

This work was financially supported by the Grant Agency of Charles University (Grant No. 318/2005/B-CH/PrF)

References

[1] (a) A. Togni, R.L. Haltermann (Eds.), Metallocenes, VCH, Weinheim, 1998;
(b) A. Togni, T. Hayashi (Eds.), Ferrocenes – Homogenous Catalysis, Organic Synthesis, Materials Science, VCH, Weinheim, 1995;
(c) C.J. Richards, A.J. Locke, Tetrahedron: Asymm. 9 (1998) 2377;
(d) T.J. Colacot, Chem. Rev. 103 (2003) 3101.
[2] R.C.J. Atkinson, V.C. Gibson, N.J. Long, Chem. Soc. Rev. 33 (2004) 313.
[3] J. Podlaha, P. Štěpnička, I. Císařová, J. Ludvík, Organometallics 15 (1996) 543.
[4] A. Bader, E. Lindner, Coord. Chem. Rev. 108 (1991) 27.
[5] (a) P. Štěpnička, R. Gyepes, O. Lavastre, P.H. Dixneuf, Organometallics 16 (1997) 5089;
(b) P. Štěpnička, J. Podlaha, R. Gyepes, M. Polášek, J. Organomet. Chem. 552 (1998) 293;
(c) P. Štěpnička, R. Gyepes, J. Podlaha, Collect. Czech. Chem. Commun. 63 (1998) 64;
(d) P. Štěpnička, I. Císařová, J. Podlaha, J. Ludvík, M. Nejezchleba, J. Organomet. Chem. 582 (1999) 319;
(e) J. Pinkas, Z. Bastl, M. Šlouf, J. Podlaha, P. Štěpnička, New J. Chem. 25 (2001) 1215;
(f) L. Lukešová, J. Ludvík, I. Císařová, P. Štěpnička, Collect. Czech. Chem. Commun. 65 (2000) 1897.
[6] K. Mach, J. Kubišta, I. Císařová, P. Štěpnička, Acta Crystallogr. C58 (2002) m116.
[7] P. Štěpnička, I. Císařová, J. Chem. Soc., Dalton Trans. (1998) 2807.
[8] P. Štěpnička, M. Lamač, I. Císařová, Polyhedron 23 (2004) 921.
[9] P. Štěpnička, J. Demel, J. Čejka, J. Mol. Catal. A: Chem. 224 (2004) 161.
[10] P. Štěpnička, New J. Chem. 26 (2002) 567.
[11] (a) J.M. Longmire, B. Wang, X. Zhang, Tetrahedron Lett. 41 (2000) 5435;
(b) S.-L. You, X.-L. Hou, L.-X. Dai, B.-X. Cao, J. Sun, Chem. Commun. (2000) 1933;
(c) Deng, X.-L. Hou, L.-X. Dai, J. Organomet. Chem. 637–639 (2001) 845.
[12] (a) Deng, X.-L. Hou, L.-X. Dai, J. Organomet. Chem. 637–639 (2001) 762;
(b) S.-L. You, X.-L. Hou, L.-X. Dai, X.-Z. Zhu, Org. Lett. 3 (2001) 149;
(c) J.M. Longmire, B. Wang, X. Zhang, J. Am. Chem. Soc. 124 (2002) 13400;
(d) B. Breit, D. Breuninger, J. Am. Chem. Soc. 126 (2004) 10244.
[13] P. Štěpnička, I. Císařová, Organometallics 22 (2003) 1728.
[14] P. Štěpnička, I. Císařová, Z. Anorg. Allg. Chem. 630 (2004) 1321.
[15] P. Štěpnička, Inorg. Chem. Commun. 7 (2004) 426.
[16] L. Xiao, K. Mereiter, W. Weissensteiner, M. Widhalm, Synthesis (1999) 1354.
[17] M. Widhalm, U. Nettekoven, K. Mereiter, Tetrahedron: Asymm. 10 (1999) 4369.
[18] G. Marr, R.E. Moore, B.W. Rockett, J. Chem. Soc. Sect. C (1968) 24.
[19] A. Togni, C. Breutel, A. Schnyder, F. Spindler, H. Landert, A. Tijani, J. Am. Chem. Soc. 116 (1994) 4062, For other examples, see [1].
[20] W.R. Cullen, E.B. Wickenheiser, Can. J. Chem. 68 (1990) 705.
[21] R. Šebesta, Ph.D. Thesis, Comenius University, Bratislava, Slovakia, 2003.
[22] H.-O. Kalinowski, S. Berger, S. Braun, ^{13}C-NMR-Spektroskopie, Thieme, Stuttgart, 1984, pp. 199–200, 530–538.

[23] N.J. Goodwin, W. Henderson, B.K. Nicholson, Inorg. Chim. Acta 295 (1999) 18.
[24] (a) M. Cais, M.S. Lupin, in: F.G.A. Stone, R. West (Eds.), Adv. Organomet. Chem., Academic Press, New York, 1970, pp. 211–333;
(b) A. Mandelbaum, M. Cais, Tetrahedron Lett. (1964) 3847;
(c) D.T. Roberts Jr., W.L. Little, M.M. Bursey, J. Am. Chem. Soc. 89 (1967) 6156.
[25] M. Polášek, P. Štěpnička, J. Mass. Spectrom. 33 (1988) 739.
[26] (a) D.H. Williams, R.S. Ward, R.G. Cooks, J. Am. Chem. Soc. 90 (1968) 966;
(b) K.A. Asker, A.M. Greenway, K.R. Seddon, A.A. Shimran, J. Organomet. Chem. 354 (1998) 257.
[27] P. Štěpnička, I. Císařová, New J. Chem. 26 (2002) 1389.
[28] P. Štěpnička, T. Baše, Inorg. Chem. Commun. 4 (2001) 682.
[29] M.C. Etter, J.C. MacDonald, Acta Crystallogr. B46 (1990) 256.
[30] Complex **11** possesses a stereogenic rhodium atom and, hence, it should give rise to a mixture of two diastereoisomeric pairs: $(R_{Rh},S_p)/(S_{Rh},R_p)$ and $(R_{Rh},R_p)/(S_{Rh},S_p)$, observable in NMR spectra.
[31] (a) A. Jegorov, B. Kratochvíl, V. Langer, J. Podlahová, Inorg. Chem. 23 (1984) 4288;
(b) A. Jegorov, J. Podlaha, J. Podlahová, F. Tureček, J. Chem. Soc., Dalton Trans. (1990) 3259.
[32] P.S. Pregosin, R.W. Kunz, ^{31}P and ^{13}C NMR Data of Transition Metal Phosphine Complexes, in NMR Basic Principles and Progress, Springer, Berlin, 1979, see also data in [7,32].
[33] D. Cremer, J.A. Pople, J. Am. Chem. Soc. 97 (1975) 1354.
[34] D. Lednicer, C.R. Hauser, in: H.E. Baumgarten (Ed.), Org. Synth., Coll., 5, Wiley, New York, 1973, pp. 434–436.
[35] C. White, D. Yates, P.M. Maitlis, in: R.N. Grimes (Ed.), Inorg. Synth., 13, McGraw-Hill, New York, 1972, pp. 47–55.
[36] Z. Otwinowski, W. Minor, HKL DENZO and SCALEPACK Program Package, Nonius BV, Delft, The Netherlands, 1997;
For a reference, see: Z. Otwinowski, W. Minor, Meth. Enzymol. 276 (1997) 307.
[37] R.H. Blessing, J. Appl. Crystallogr. 30 (1997) 421.
[38] A. Altomare, M.C. Burla, M. Camalli, G.L. Cascarano, C. Giacovazzo, A. Guagliardi, A.G.G. Moliterni, G. Polidori, R. Spagna, J. Appl. Crystallogr. 32 (1999) 115.
[39] G.M. Sheldrick, SHELXL97, Program for Crystal Structure Refinement from Diffraction Data, University of Göttingen, Germany, 1997.
[40] A.L. Spek, PLATON A Multipurpose Crystallographic Tool, Utrecht University, The Netherlands, 2003. Available from: <http://www.cryst.chem.uu.nl/platon/> .